Tipping Points

G14PJS

Mathematics 3rd Year Project

Spring 2017/18

School of Mathematical Sciences

University of Nottingham

Jack Davies

Supervisor: Dr S. M. Cox

Project Code: SMC P1

Assessment Type: Investigation

I have read and understood the School and University guidelines on plagiarism. I confirm that this work is my own, apart from the acknowledged references.

Abstract

The aim of this project is to introduce the reader to rate-dependent tipping phenomena. This occurs in non-autonomous systems when a time-dependent parameter changes rapidly, causing the system to destabilise and change behaviour as a result. This change in behaviour is due to trajectories not being able to keep up with a moving branch of attractors. Such destabilisation is referred to as the system 'tipping'. We shall consider several models exhibiting this non-autonomous instability and analyse them to identify the rate of parameter variation which induces this tipping behaviour. In particular, we will analyse bifurcation models and fast-slow dynamical systems to motivate this material. An alternative approach to analysing rate-dependent tipping, which involves finding a so called tipping radius, will also be discussed.

Contents

1 Introduction

Critical transitions or '**tipping points**' for dynamical systems are where systems undergo a sudden and irreversible change in behaviour in response to some parameter shift. Such critical transitions cause systems to destabilise and force trajectories to move towards somewhere distant in phase space. Such tipping points are considered in many different applications, including: climate science [15], ecology, neuroscience and physics [6, p. 3-5].

There are many different types of tipping mechanisms [6, p. 2-3], such as bifurcation-induced tipping (B-tipping), where a branch of attractors becomes unstable in a bifurcation, and noise-induced tipping (N-tipping), where the presence of noise [12, p. 1-2] results in the system moving away from a branch of attractors [2, 1167-1168]. In this project, we will focus our attention on a particular class of tipping phenomena, namely **rate-dependent tipping** or **R-tipping**. This phenomena occurs not as a consequence of varying a parameter, but rather as a consequence of changing a parameter rapidly. It turns out that if you vary a parameter fast enough, this can result in a system not being able to keep up with a continuously changing branch of attractors. This can force the system to move to somewhere distant in the phase space as a consequence of trajectories no longer being within the moving branch of attractors basin of attraction.

To begin with, the first half of section 2 reviews the theory of linear stability in one and two dimensions. Criteria for whether an equilibrium point is stable or unstable will be derived and the behaviour of trajectories near different types of equilibria will be discussed. In the second half of section 2, we will introduce the reader to some elementary bifurcation theory. This will include an introduction to the saddle-node bifurcation and the Hopf bifurcation.

In section 3, we will model rate-dependent tipping generally by a non-autonomous ordinary differential equation, with time-dependent external conditions, $\boldsymbol{\lambda}(t)$. We say that if the system has a stable equilibrium point, $\boldsymbol{y}_e^s(\boldsymbol{\lambda})$, when $\dot{\boldsymbol{\lambda}} = 0$, then the system has time-dependent quantity $\boldsymbol{y}_e^s(\boldsymbol{\lambda}(t))$ when $\dot{\boldsymbol{\lambda}} \neq 0$. We call this time-dependent quantity a **quasi-static attractor**, and assume that trajectories for the system roughly approach (track) this quantity.

Thus, the system tips if it fails to track the quasi-static attractor. The rest of this section concerns itself with finding criteria for a linear system to tip in terms of a **tipping radius**. This is the distance between the system and the quasi-static attractor, that if exceeded, forces the system to tip.

In the remaining sections, we will present examples of different models exhibiting rate-dependent tipping phenomena. It turns out that for all the models considered, one can either find exactly, or find an approximation for a rate of change of parameter shift, which if exceeded, forces the system to tip. The aim of these sections is to find the rate of change of parameter shift which induces rate-dependent tipping. In Section 4, we analyse rate-dependent tipping in a saddle-node normal form, where the motion of the quasi-static attractor is uniform. We do the same in section 5 for a subcritical Hopf normal form, but also briefly consider when the motion of the quasi-static attractor is non-uniform.

Finally, we conclude the project with section 6, where we consider a system with both a fast and slow time-scale. The behaviour of such systems can be difficult to analyse exactly, but can be approximated by considering what happens when the ratio of time-scales, ε, tends to zero. This gives us an approximation for the (slow) dynamics of the system, and so we can use this to approximate a rate of parameter shift, which if exceeded, induces rate-dependent tipping. Approximations will be given for both uniform and non-uniform movement of the quasi-static attractor.

Remark. *The notation [S, P] has been used throughout this introduction. We will use this notation throughout the project to cite pages from different sources. In this notation, S represents the source and P represents the relevant pages. If the source only has relevant pages, then we will cite the source without page numbers. In the instance we wish to be more specific when citing sources, we will use a third argument in our notation. This will normally involve some form of labelling, such as an equation number of theorem number.*

2 Elementary Bifurcation Theory

Before we can begin investigating rate-dependent tipping, we must first review some fundamental material that will prove useful. The topics we will discuss here will help us understand the dynamics of systems exhibiting this tipping behaviour later on. The first half of this section will remind the reader of how to analyse the stability of equilibrium points by means of **linearisation**. We include this material here since it will be used throughout the project. The second half will introduce the reader to some elementary bifurcation theory. This subject on its own is very broad, so for simplicity, we will only introduce concepts which will be used later on (see sections 4 and 5).

2.1 A Review of Linear Stability

2.1.1 One Dimensional Systems

Suppose that we have the differential equation

$$\frac{dx}{dt} = f(x,t). \tag{2.1}$$

Definition 2.1. *Equation* (2.1) *is referred to as* ***autonomous*** *if it does not depend explicitly on the independent variable i.e.* $\dot{x} = g(x)$.

Autonomous equations are nice since we can learn how the system behaves by drawing a phase line (or phase plane in two dimensions) [13, p. 222–223]. In order to draw these diagrams, we need to find the systems **equilibrium points**:

Definition 2.2. *An* ***equilibrium point*** *of* (2.1), $x = x_e$, *is a solution to the equation* $\dot{x} = 0$.

If instead, we prefer an algebraic approach to analysing the systems behaviour, we can rely on linearisation. Suppose that the nonlinear autonomous ordinary differential equation $\dot{x} = g(x)$ has an equilibrium point at $x = x_e$. Then, if we set $x(t) = x_e + x_1(t)$, where $x_1(t) \ll 1$, then

we can Taylor expand g near the equilibrium point to obtain

$$g(x_e + x_1) = g(x_e) + x_1 g'(x_e) + \ldots \approx x_1 g'(x_e), \tag{2.2}$$

since $g(x_e) = 0$ and higher order terms in x_1 are so small they can be considered negligible. So near the equilibrium point, we have the linear system

$$\frac{dx_1}{dt} = x_1 g'(x_e), \tag{2.3}$$

which has exponential solutions

$$x_1(t) = Ae^{g'(x_e)t} \tag{2.4}$$

for some arbitrary constant A. From this result, we can see that[1]

- if $g'(x_e) < 0$, then $x_1(t) \to 0$ as $t \to \infty$. In this case, we call the equilibrium point **stable**.
- if $g'(x_e) > 0$, then $x_1(t) \to \infty$ as $t \to \infty$. In this case, we call the equilibrium point **unstable**.

2.1.2 Two Dimensional Systems

We can extend this stability analysis to two dimensional systems and beyond. For example, suppose that we have a nonlinear autonomous system

$$\frac{dx}{dt} = f(x, y), \quad \frac{dy}{dt} = g(x, y), \tag{2.5}$$

with solutions (or trajectories) $(x(t), y(t))$.

Definition 2.3. *If $f(x_e, y_e) = g(x_e, y_e) = 0$, then the solution (x_e, y_e) is called an **equilibrium point** of the nonlinear system (2.1).*

[1] In the event that $g'(x_e) = 0$, then linearisation does not tell us how the system behaves and we need to consider nonlinear terms in the Taylor expansion for g.

To get an understanding of how trajectories behave near an equilibrium point, we can linearise the system similar to before. If we set $x(t) = x_e + x_1(t)$ and $y(t) = y_e + y_1(t)$, where (x_e, y_e) is an equilibrium point and $x_1(t), y_1(t) \ll 1$, then Taylor expanding f and g near the equilibrium point yields

$$\begin{aligned} f(x,y) &\approx x_1 \frac{\partial f}{\partial x}(x_e, y_e) + y_1 \frac{\partial f}{\partial y}(x_e, y_e), \\ g(x,y) &\approx x_1 \frac{\partial g}{\partial x}(x_e, y_e) + y_1 \frac{\partial g}{\partial y}(x_e, y_e), \end{aligned} \tag{2.6}$$

where we have made use of $f(x_e, y_e) = g(x_e, y_e) = 0$ and have chosen to neglect higher order terms since they are very small in comparison to the initial terms in the expansion. By expressing this in matrix form, the linear system near the equilibrium point becomes

$$\frac{d\boldsymbol{x}}{dt} = \boldsymbol{J}(x_e, y_e)\boldsymbol{x}, \tag{2.7}$$

where $\boldsymbol{x} = (x_1, y_1)$ and

$$\boldsymbol{J}(x_e, y_e) = \begin{bmatrix} \frac{\partial f}{\partial x}(x_e, y_e) & \frac{\partial f}{\partial y}(x_e, y_e) \\ \frac{\partial g}{\partial x}(x_e, y_e) & \frac{\partial g}{\partial y}(x_e, y_e) \end{bmatrix}. \tag{2.8}$$

The matrix $\boldsymbol{J}$ is better known as the Jacobian matrix for the linearised system. From this, if we seek exponential solutions of the form

$$\boldsymbol{x}(t) = \boldsymbol{w}e^{\gamma t}, \tag{2.9}$$

where $\boldsymbol{w}$ is a nonzero constant vector and γ is a constant scalar, then we obtain

$$\big[\boldsymbol{J}(x_e, y_e) - \gamma \mathbb{I}\big]\boldsymbol{w} = \boldsymbol{0}, \tag{2.10}$$

with $\mathbb{I}$ and $\boldsymbol{0}$ denoting the 2×2 identity matrix and 2×1 zero vector respectively. So our differential equation has been reduced to an eigenvalue problem. Clearly, the matrix

$\left[\boldsymbol{J}(x_e, y_e) - \gamma\mathbb{I}\right]$ is singular, otherwise $\boldsymbol{w} = \boldsymbol{0}$, which contradicts our choice of $\boldsymbol{w}$. As a consequence of this [18, p. 272], we have

$$\det\left[\boldsymbol{J}(x_e, y_e) - \gamma\mathbb{I}\right] = 0, \tag{2.11}$$

which has eigenvalue solutions

$$\gamma_\pm = \frac{1}{2}\left[\operatorname{tr}\boldsymbol{J}(x_e, y_e) \pm \sqrt{\operatorname{tr}^2\boldsymbol{J}(x_e, y_e) - 4\det\boldsymbol{J}(x_e, y_e)}\,\right], \tag{2.12}$$

with tr denoting the trace and tr^2 denoting the square of the trace. Since we want solutions for a linear equation, the general solution is the linear combination

$$\boldsymbol{x}(t) = A\boldsymbol{w}_+ e^{\gamma_+ t} + B\boldsymbol{w}_- e^{\gamma_- t}, \tag{2.13}$$

where $\boldsymbol{w}_\pm$ are the solutions to the eigenvalue problem with $\gamma = \gamma_\pm$ and A, B are arbitrary constants. We call $\boldsymbol{w}_\pm$ the eigenvectors which correspond to the eigenvalues.

Since we have exponential solutions, the stability for the system depends on the eigenvalues of the Jacobian matrix. However, these are solutions for the linearisation, which means we are neglecting nonlinear terms. For some equilibrium points, the stability remains the same, but for others, the stability is different in the full nonlinear system. Whether the nonlinear terms are important or not when it comes to identifying stability depends on the type of equilibrium point we are working with.

Definition 2.4. *An equilibrium point is said to be* ***hyperbolic*** *if* $\mathbb{R}e(\gamma_\pm) \neq 0$.

This class of equilibrium point exhibits different stability depending on the value of $\mathbb{R}e(\gamma_\pm)$. We can summarise the behaviour of trajectories near such points as follows:

- **Nodes**: these are equilibrium points where the eigenvalues are real, distinct and have the same sign in common. If the sign is negative, then we have a stable node and

if the sign is positive, we have an unstable node. Graphical representations of these equilibrium points are given in figure 2.1.

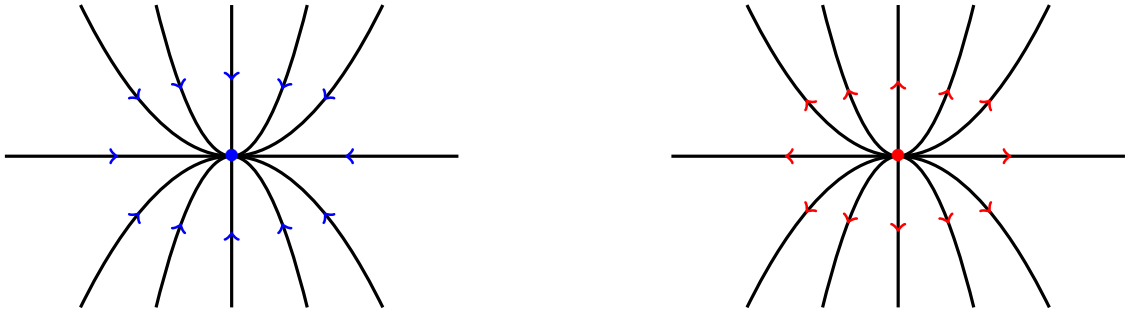

Figure 2.1: Examples of phase portraits for stable and unstable nodes respectively.

- **Saddles**: these are equilibrium points where the eigenvalues are real and have opposite signs. Due to the presence of a positive eigenvalue, saddle points are unstable. A graphical representation for a saddle equilibrium is given in figure 2.2.

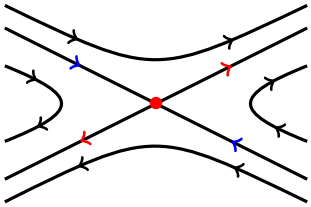

Figure 2.2: An example of a phase portrait for a saddle equilibrium point.

- **Spirals**: these are equilibrium points where the eigenvalues are complex conjugate pairs. We have a stable spiral when the eigenvalues have positive real part and we have an unstable spiral when the eigenvalues have negative real part. Graphical representations of stable and unstable spirals are given in figure 2.3.

Since eigenvalues are related to the trace and determinant of the Jacobian matrix by (2.12), we can rewrite our criteria for classifying equilibrium points in terms of the trace and determinant

Figure 2.3: Examples of phase portraits for stable and unstable spirals respectively.

if we so choose (in some cases, this might be more convenient). Hyperbolic equilibrium points are nice because the **Hartman-Grobman Theorem** [13, p. 230] tells us that the behaviour found from the linearised system is consistent with the behaviour in the full nonlinear system in the neighbourhood of the equilibrium point. When we have **nonhyperbolic equilibrium points**, analysis of nonlinear terms is required to understand the complete behaviour near the equilibrium point. Examples of such equilibria include:

- **Lines of equilibria**: these are equilibrium points where there is a zero eigenvalue. In the case the second eigenvalue is negative, we say the line of equilibria is stable and in the case the eigenvalue is positive, we say the line of equilibria is unstable. Graphical representations of lines of equilibria are given in figure 2.4.

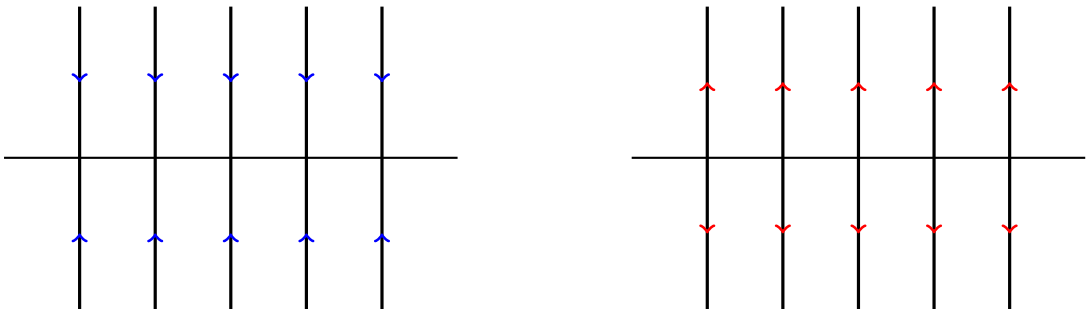

Figure 2.4: Examples of phase portraits for stable and unstable lines of equilibria respectively.

- **Centres**: these are equilibrium points where the eigenvalues are purely imaginary. Graphical representations of centres are given in figure 2.5.

Figure 2.5: Examples of phase portraits for centres.

In the instance we have a zero eigenvalue, there are theorems such as the **Centre Manifold Theorem** [5, p. 281] which can be used to identify the complete behaviour of trajectories near nonhyperbolic equilibrium points.

2.2 Destabilising an Equilibrium Point

Systems of differential equations can be very sensitive to parameter shifts. A subtle variation in the value of a parameter can be the catalyst for the destruction or creation of equilibrium points, or even a change in the associated stability for these equilibrium points. Such a change can lead to systems exhibiting different dynamics. We call this qualitative change in behaviour a **bifurcation** and the parameter which induces this change a **bifurcation point**.

To put this into perspective, suppose you place a weight on a diving board. If the weight is relatively light, then the diving board will remain horizontal. However, if the weight is heavy enough, the diving board will bend and eventually break. In other words, the stability of the diving board has gone from being stable to unstable due to a change in weight acting on it. The change in weight is the parameter shift in the system and the behaviour of the diving board represents the system dynamics. The bifurcation point associated with this scenario is the weight at which the board is about to break.

In this section, we will develop our understanding of bifurcation theory by considering some fundamental bifurcation models. This material will play a huge role later on when we come to discuss rate-dependent tipping.

2.2.1 The Saddle-Node Bifurcation

The normal form for a **saddle-node bifurcation** in one dimension is given by

$$\frac{dy}{dt} = y^2 - \mu = f(y;\mu), \tag{2.14}$$

where $y \in \mathbb{R}$, the real number μ is a variable parameter and t represents time. We refer to (2.14) as the normal form because if we linearise the system near the saddle-node bifurcation point, we can always express the system in this particular form.

Since the equilibrium points for the system are given by $y^2 = \mu$, we see that the number of equilibrium points changes depending on μ. When $\mu > 0$, there are two hyperbolic equilibrium points, namely $y_\pm = \pm\sqrt{\mu}$. When $\mu = 0$, the equilibrium points coalesce into a single **half stable** [22, p. 46] equilibrium point at $y = 0$. When $\mu < 0$, the equilibrium points vanish. Since there is an obvious change in the number of solutions when μ passes through zero, $\mu = 0$ is a bifurcation point for the system. We can summarize these cases with the phase lines illustrated in figure 2.6.

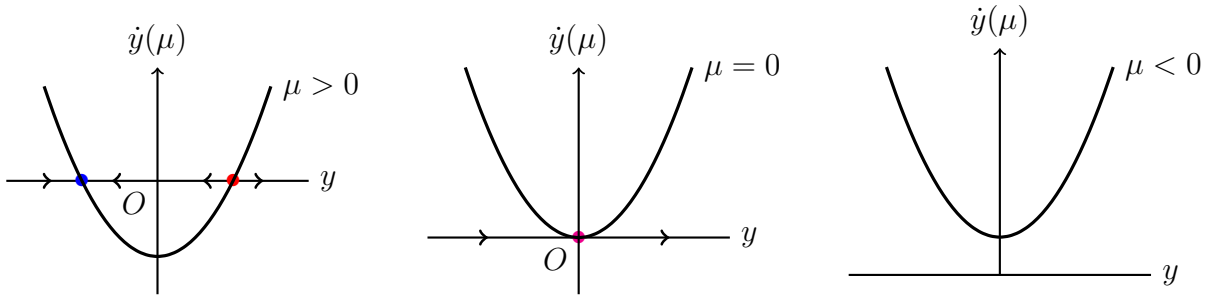

Figure 2.6: Phase lines for (2.14) when $\mu < 0$, $\mu = 0$ and $\mu > 0$.

A convenient way to identify the position and stability of equilibrium points as a function of the bifurcation parameter μ is by drawing a bifurcation diagram. Such diagrams are obtained by sketching the equilibrium solutions for the system. In this case, these solutions are $y = \pm\sqrt{\mu}$. The solution $y = -\sqrt{\mu}$ is a stable equilibrium point (see the phase line for $\mu > 0$) and so the vertical lines point towards this curve. In a similar way, the solution

$y = \sqrt{\mu}$ is an unstable equilibrium point and so the vertical lines point away from this curve.

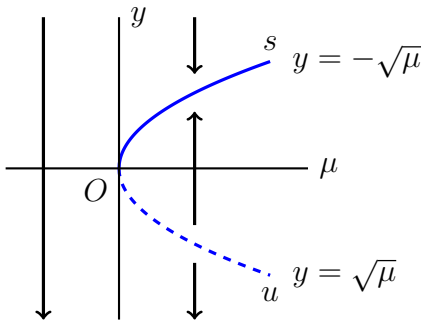

Figure 2.7: Bifurcation diagram for (2.14).

2.2.2 The Hopf Bifurcation

Let us turn our attention to a two-dimensional system with a stable equilibrium point. We have already seen the influence a varying parameter μ has on the stability and number of equilibrium points for a one-dimensional system. To understand the effects of this variation in two-dimensions, we must consider the eigenvalues of the Jacobian matrix for the linearised equations. For a stable equilibrium point, we have eigenvalues γ such that $\mathbb{R}e(\gamma) < 0$. This can be visualised in the complex plane as the eigenvalues being restricted to the left half-plane. In two dimensions, the eigenvalues are solutions to a quadratic equation. This tells us that we either have eigenvalues that are both real and negative, or we have eigenvalues that are a pair of complex conjugates, γ and $\bar{\gamma}$ (where $\bar{\gamma}$ is used to represent the complex conjugate of γ). For the system to have a bifurcation, we need the stability of the system to change in response to a parameter variation. Visually, this corresponds to one or both eigenvalues moving from the left half-plane to the right half-plane.

In this section, we will focus on the case where the eigenvalues associated with equilibrium points for the system are complex conjugates. We say that a **Hopf bifurcation** occurs when these eigenvalues cross the imaginary axis as a result of a parameter variation. Visually, this

might look something along the lines of what can be seen in figure 2.8.

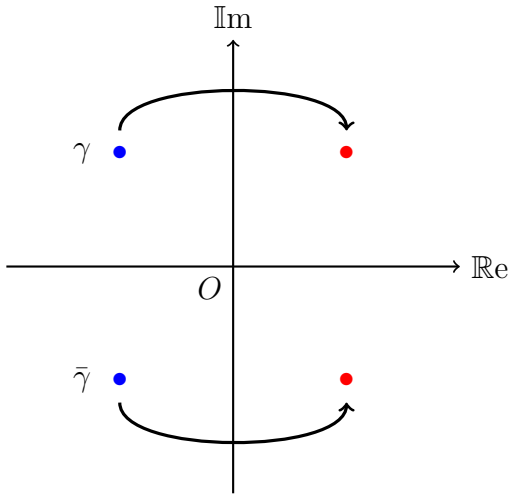

Figure 2.8: Eigenvalues crossing the imaginary axis as a result of parameter variation.

It turns out that the normal form for a Hopf bifurcation is more compact in polar coordinates. There are two types of Hopf bifurcation, namely the **supercritical** bifurcation with normal form

$$\frac{dr}{dt} = \mu r - r^3, \quad \frac{d\theta}{dt} = \omega, \tag{2.15}$$

and the **subcritical** bifurcation with normal form

$$\frac{dr}{dt} = \mu r + r^3, \quad \frac{d\theta}{dt} = \omega. \tag{2.16}$$

In both instances, ω denotes the angular frequency. In the case we have constant solutions for r, this corresponds to limit cycles in phase space (closed, periodic curves).

Let us consider the subcritical Hopf bifurcation with normal form (2.16). It is clear that the system has equilibrium points given by $\dot{r} = 0$, that is

$$\mu r + r^3 = 0 \implies r(\mu + r^2) = 0. \tag{2.17}$$

Clearly, the number of equilibrium points changes depending on the value of μ. So we must

consider the various cases separately:

- If $\mu < 0$, we can write $\mu = -k^2 < 0 \ \forall k \in \mathbb{R}$. Using this change of variables, equation (2.17) can be rewritten as

$$r(r^2 - k^2) = 0. \tag{2.18}$$

From this, we must have equilibria defined by $r = 0$ and $r = \sqrt{k}$. The corresponding phase line is illustrated in figure 2.9.

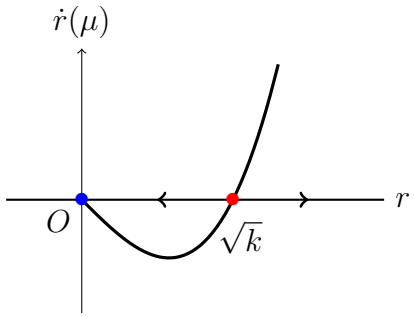

Figure 2.9: Phase line for (2.18).

From figure 2.9, we can see that the origin defined by $r = 0$ is a stable equilibrium point and $r = \sqrt{k}$ is an unstable equilibrium point. Since the eigenvalues for these equilibria are complex conjugates, we must have complex spirals. Thus, $r = 0$ is a stable spiral and $r = \sqrt{k}$ is an unstable limit cycle. Visually, this looks something along the lines of figure 2.10.

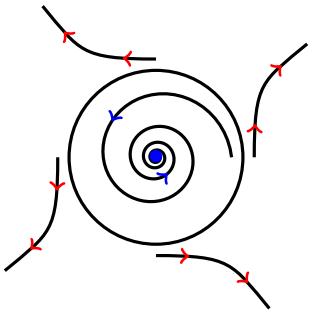

Figure 2.10: An illustration of a stable spiral at $r = 0$ and an unstable limit cycle at $r = \sqrt{k}$.

- If $\mu > 0$, then a sketch of the phase line reveals the origin to be an unstable spiral and that there is no limit cycle.

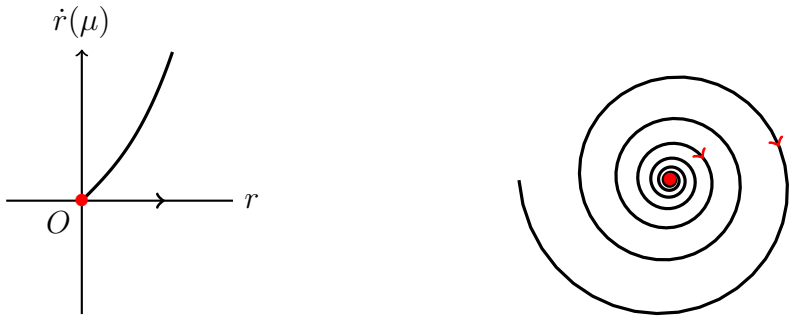

Figure 2.11: Illustrations of the phase line and unstable spiral for $\mu > 0$.

Therefore, from our analysis, we can deduce that there is a Hopf bifurcation at $\mu = 0$.

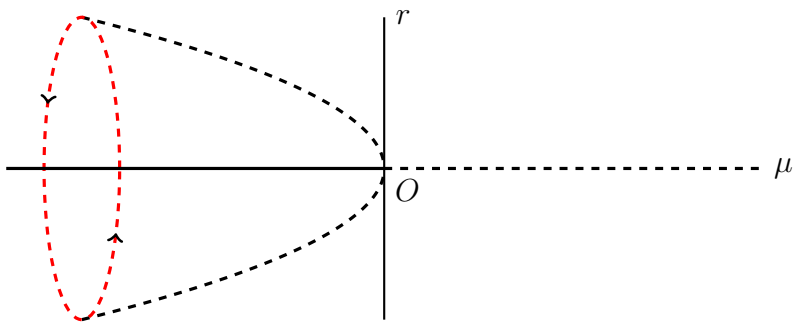

Figure 2.12: The bifurcation diagram for (2.16), where unstable equilibria are denoted by dashed lines, stable equilibria are denoted by thick lines, and the dashed circle with arrows on denotes the limit cycle born from the subcritical Hopf bifurcation.

Remark. *It can sometimes be very difficult to identify whether we have a subcritical or supercritical Hopf bifurcation since linearisation does not provide us with an obvious distinction. It can also be challenging to identify the stability associated with limit cycles which correspond to Hopf bifurcations. To overcome this difficulty, we can make use of theorems such as the* ***Hopf bifurcation Theorem*** *[13, p. 403-405] to identify the type of Hopf bifurcation and the stability of the limit cycles born from the Hopf bifurcation.*

3 An Introduction to R-Tipping Phenomena

3.1 An Arbitrary Construction

The main focus of this project is to analyse the phenomenon of **rate-dependent tipping** or **R-tipping** in a variety of different systems. To do this for some arbitrary system, we must first encompass this behaviour into our model approximation. If we assume that environmental factors can be approximated by sufficiently smooth, time evolving functions $\boldsymbol{\lambda}(t)$, then a generalised model for rate-dependent tipping could take the form

$$\frac{d\boldsymbol{y}}{dt} = \boldsymbol{f}(\boldsymbol{y}, \boldsymbol{\mu}, \boldsymbol{\lambda}(t)), \tag{3.1}$$

where $\boldsymbol{y} \in \mathbb{R}^\ell$ is the position vector, $\boldsymbol{f} \in \mathbb{R}^\ell$ is a vector of sufficiently smooth functions, $\boldsymbol{\mu} \in \mathbb{R}^m$ is a vector of time-independent parameters, $\boldsymbol{\lambda} \in \mathbb{R}^n$ is a vector of external conditions and $t \geq 0$ denotes time ($\ell, m, n \in \mathbb{N}$).

Since this system is not autonomous, we can no longer rely on equilibrium points to describe the dynamics. The reason for this is that $\dot{\boldsymbol{y}}$ can now depend explicitly on time, so even if we are initially positioned somewhere satisfying $\dot{\boldsymbol{y}} = \boldsymbol{0}$, as time passes, the value of $\dot{\boldsymbol{y}}$ can change. Moreover, different positions might satisfy $\dot{\boldsymbol{y}} = \boldsymbol{0}$ at different times as a consequence of this explicit time dependence. This idea motivates the following definition:

Definition 3.1. *When $\dot{\boldsymbol{\lambda}} = \boldsymbol{0}$, the system (3.1) has equilibrium point $\boldsymbol{y}_e(\boldsymbol{\lambda})$. When $\dot{\boldsymbol{\lambda}} \neq \boldsymbol{0}$, then we define the **quasi-static equilibrium** to be the time-dependent quantity $\boldsymbol{y}_e(\boldsymbol{\lambda}(t))$.*

In particular, if $\boldsymbol{y}_e(\boldsymbol{\lambda})$ is stable, then we call the quasi-static equilibrium a **quasi-static attractor** and denote it by $\boldsymbol{y}_e^s(\boldsymbol{\lambda}(t))$. Similarly, if $\boldsymbol{y}_e(\boldsymbol{\lambda})$ is unstable, then we call the quasi-static equilibrium a **quasi-static repeller** and denote it by $\boldsymbol{y}_e^u(\boldsymbol{\lambda}(t))$.

A geometric interpretation of our definition for a quasi-static equilibrium is relating it to the notion of a moving equilibrium point constantly shifting to different positions in phase space. It is worth noting that the quasi-static equilibrium is not in general an equilibrium

point. If $\boldsymbol{\lambda}$ is constant in time, then the quasi-static equilibrium reduces to an equilibrium point for the system. As a consequence of $\boldsymbol{\lambda}$ being time-dependent, we only expect trajectories to **track** (roughly approach) the quasi-static attractors for the system. In other words, we can use quasi-static attractors to approximate the dynamics of a non-autonomous system.

If $\boldsymbol{\lambda}$ evolves slowly in time, then trajectories will continue to track $\boldsymbol{y}_e^s(\boldsymbol{\lambda}(t))$ if they are initially positioned in some local neighbourhood of $\boldsymbol{y}_e^s(\boldsymbol{\lambda}(t))$. It turns out that if $\boldsymbol{\lambda}$ evolves fast enough, then trajectories which are initially close to $\boldsymbol{y}_e^s(\boldsymbol{\lambda}(t))$ may no longer be able to keep up with the quasi-static attractor and the system might **destabilise** as a result. The new behaviour for the trajectories will depend on the other types of stability that are present in the system. It could be the case that this destabilisation takes the form of trajectories diverging from $\boldsymbol{y}_e^s(\boldsymbol{\lambda}(t))$ and tracking some other quasi-static attractor. We could have trajectories diverging and moving freely due to no other stability existing in the system. Or perhaps trajectories diverge and then return to track $\boldsymbol{y}_e^s(\boldsymbol{\lambda}(t))$.

From this discussion, we can assume that there exists some rate $\xi > 0$, that if exceeded, forces the system to tip and exhibit a qualitative change in behaviour. We shall refer to this value as the **critical threshold** for which rate-dependent tipping occurs and denote it by ξ_c. Obviously, if we can identify the critical threshold for different systems, we have a way to avoid rate-dependent tipping, or at least understand the conditions for which rate-dependent tipping takes place. However, there are various other approaches to this subject. In a recent paper by Ashwin [1], systems with rate-dependent tipping were analysed by considering **local pullback attractors**. Another approach is to find the distance between the system and the quasi-static attractor, which if exceeded, induces rate-dependent tipping. This distance is called the **tipping radius** for the system, and the rest of this section concerns itself with expanding on this tipping radius approach.

3.2 A Linear Model with Tipping Radius

Working with an arbitrarily high dimensional system is not often ideal since it can be difficult to make progress mathematically. To avoid this difficulty, let us consider the reduced system

$$\frac{d\boldsymbol{y}}{dt} = \boldsymbol{f}(\boldsymbol{y}, \lambda), \tag{3.2}$$

where $\boldsymbol{y} \in \mathbb{R}^n$ and $\lambda \in \mathbb{R}$ is an arbitrary parameter. Suppose that the system has stable equilibrium point $\boldsymbol{y}_e^s(\lambda)$ and some **stable region** defined by a fixed **tipping radius** $r > 0$ for which the behaviour of trajectories remains the same. If we are initially positioned in the stable region, that is we have initial positions $\boldsymbol{y}_0$ satisfying $\big|\big|\boldsymbol{y}_0 - \boldsymbol{y}_e^s(\lambda)\big|\big| < r$, then we will assume that we can describe the time evolution of $\boldsymbol{y}$ by

$$\frac{d\boldsymbol{y}}{dt} = \boldsymbol{\Omega}\big[\boldsymbol{y} - \boldsymbol{y}_e^s(\lambda)\big] \quad \text{for} \quad \big|\big|\boldsymbol{y} - \boldsymbol{y}_e^s(\lambda)\big|\big| < r, \tag{3.3}$$

where $\boldsymbol{\Omega}$ is some $n \times n$ constant stable linear operator i.e. $\big|\big|e^{\boldsymbol{\Omega} t}\big|\big| \to 0$ as $t \to \infty$, with matrix exponential defined by

$$e^{\boldsymbol{\Omega} t} = \sum_{j=0}^{\infty} \frac{(\boldsymbol{\Omega} t)^j}{j!} = \mathbb{I} + \boldsymbol{\Omega} t + \frac{1}{2}(\boldsymbol{\Omega} t)^2 + \cdots, \tag{3.4}$$

where $\mathbb{I}$ represents the $n \times n$ identity matrix. To make this model approximation more realistic, let us allow λ to evolve as a function of time. As a consequence of λ evolving in time, the system is no longer autonomous, so instead of having a stable equilibrium point, the system has quasi-static attractor $\boldsymbol{y}_e^s(\lambda(t))$. If $\big|\big|\boldsymbol{y}(t) - \boldsymbol{y}_e^s(\lambda(t))\big|\big| < r$, then the trajectory $\boldsymbol{y}(t)$ tracks or **adiabatically**[2] follows $\boldsymbol{y}_e^s(\lambda(t))$, whereas, if $\exists t_0$ s.t. $\big|\big|\boldsymbol{y}(t_0) - \boldsymbol{y}_e^s(\lambda(t_0))\big|\big| \geq r$, then the system tips. In this case, we say that the **adiabatic approximation** fails at t_0. If such a t_0 exists, we can conclude that the model is not physically accurate beyond this point

[2]The term **adiabatic** refers to external conditions changing so slowly that we are still able to approximate the dynamics of the system with a quasi-static attractor.

in time.

Imposing the initial condition $\boldsymbol{y}(t_0) = \boldsymbol{y}_0$, we can solve the system of first order linear ordinary differential equations by finding an integrating factor [20, p. 473-474]. The simplest choice of integrating factor turns out to be

$$\boldsymbol{I}(t) = e^{\int -\boldsymbol{\Omega} dt} = e^{-\boldsymbol{\Omega} t}. \tag{3.5}$$

Rearranging the system defined in (3.3) and multiplying both sides by $\boldsymbol{I}(t)$ gives us

$$\begin{aligned} &\frac{d}{dt}(e^{-\boldsymbol{\Omega} t}\boldsymbol{y}) = -e^{-\boldsymbol{\Omega} t}\boldsymbol{\Omega}\boldsymbol{y}_e^s(\lambda) \\ \implies \quad &\boldsymbol{y}(t) = e^{\boldsymbol{\Omega}(t-t_0)}\boldsymbol{y}_0 - \int_{t_0}^{t} e^{\boldsymbol{\Omega}(t-\tau)}\boldsymbol{\Omega}\boldsymbol{y}_e^s(\lambda(\tau))d\tau. \end{aligned} \tag{3.6}$$

Now, if we assume that trajectories in our linear model are near the quasi-static attractor for an arbitrarily long past time, that is, $t - t_0 \to \infty$, then as a consequence of our definition for $\boldsymbol{\Omega}$, we can eliminate the initial value. If we write $\sigma = t - \tau$, it follows that $d\sigma = -d\tau$, so substitution yields

$$\begin{aligned} \boldsymbol{y}(t) &= \lim_{t-t_0\to\infty}\left[e^{\boldsymbol{\Omega}(t-t_0)}\boldsymbol{y}_0 - \int_{t_0}^{t} e^{\boldsymbol{\Omega}(t-\tau)}\boldsymbol{\Omega}\boldsymbol{y}_e^s(\lambda(\tau))d\tau\right] \\ &= -\int_0^{\infty} e^{\boldsymbol{\Omega}\sigma}\boldsymbol{\Omega}\boldsymbol{y}_e^s(\lambda(t-\sigma))d\sigma. \end{aligned} \tag{3.7}$$

Let us suppose further that $\boldsymbol{\Omega}$ is invertible, exponentially stable and the first and second derivatives of $\boldsymbol{y}_e^s(\lambda(t))$ and $\lambda(t)$ are bounded in time. By introducing the dummy variables $\boldsymbol{u}$ and $\boldsymbol{v}$ and setting $\boldsymbol{u} = \boldsymbol{y}_e^s(\lambda(t-\sigma))$ and $\boldsymbol{v}'(\sigma) = e^{\boldsymbol{\Omega}\sigma}\boldsymbol{\Omega}$, it follows that

$$\boldsymbol{u}'(\sigma) = -\frac{d\boldsymbol{y}_e^s}{dt}(\lambda(t-\sigma)), \;\; \boldsymbol{v} = e^{\boldsymbol{\Omega}\sigma}. \tag{3.8}$$

Thus, we can use integration by parts to obtain

$$\begin{aligned}\boldsymbol{y}(t) &= -\left[e^{\boldsymbol{\Omega}\sigma}\boldsymbol{y}_e^s(\lambda(t-\sigma))\Big|_0^\infty + \int_0^\infty e^{\boldsymbol{\Omega}\sigma}\frac{d\boldsymbol{y}_e^s}{dt}d\sigma\right] \\ &= \boldsymbol{y}_e^s(\lambda(t)) - \int_0^\infty e^{\boldsymbol{\Omega}\sigma}\frac{d\boldsymbol{y}_e^s}{dt}(\lambda(t-\sigma))d\sigma,\end{aligned} \tag{3.9}$$

which can be rewritten as

$$\boldsymbol{y}(t) - \boldsymbol{y}_e^s(\lambda(t)) = -\int_0^\infty e^{\boldsymbol{\Omega}\sigma}\frac{d\boldsymbol{y}_e^s}{dt}d\sigma. \tag{3.10}$$

If we integrate by parts again, we see that

$$\begin{aligned}\boldsymbol{y}(t) - \boldsymbol{y}_e^s(\lambda(t)) &= -\left[e^{\boldsymbol{\Omega}\sigma}\boldsymbol{\Omega}^{-1}\frac{d\boldsymbol{y}_e^s}{dt}\Big|_0^\infty + \int_0^\infty e^{\boldsymbol{\Omega}\sigma}\boldsymbol{\Omega}^{-1}\frac{d^2\boldsymbol{y}_e^s}{dt^2}d\sigma\right] \\ &= \boldsymbol{\Omega}^{-1}\frac{d\boldsymbol{y}_e^s}{dt} - \int_0^\infty e^{\boldsymbol{\Omega}\sigma}\boldsymbol{\Omega}^{-1}\frac{d^2\boldsymbol{y}_e^s}{dt^2}d\sigma.\end{aligned} \tag{3.11}$$

So we have expressed this result as a sum of two terms, namely a linear term and an error term in the form of an integral. The first term is a linear approximation for how trajectories behave in the neighbourhood of the quasi-static attractor, so we shall refer to this as the **linear instantaneous lag**:

$$\boldsymbol{\ell}(t) = \boldsymbol{\Omega}^{-1}\frac{d\boldsymbol{y}_e^s}{dt}(\lambda(t-\sigma)). \tag{3.12}$$

As a consequence of the chain rule, we can express the linear instantaneous lag as

$$\boldsymbol{\ell}(t) = \boldsymbol{\Omega}^{-1}\frac{d\boldsymbol{y}_e^s}{d\lambda}\frac{d\lambda}{dt} = \boldsymbol{\Omega}^{-1}\boldsymbol{\xi}(t), \tag{3.13}$$

where we define

$$\boldsymbol{\xi}(t) := \frac{d\boldsymbol{y}_e^s}{dt} = \frac{d\boldsymbol{y}_e^s}{d\lambda}\frac{d\lambda}{dt} \tag{3.14}$$

to be the rate of change of the quasi-static attractor. In some literature this quantity is referred to as the **quasi-static drift**. The second term is the corresponding error in this

linear approximation, so we will call this the **linear error**:

$$\boldsymbol{\epsilon}(t) = -\int_0^\infty e^{\boldsymbol{\Omega}\sigma}\boldsymbol{\Omega}^{-1}\frac{d^2\boldsymbol{y}_e^s}{dt^2}(\lambda(t-\sigma))d\sigma. \tag{3.15}$$

In a similar way to how we derived (3.13), we can rewrite the error term defined in (3.15) as

$$\boldsymbol{\epsilon}(t) = -\int_0^\infty e^{\boldsymbol{\Omega}\sigma}\boldsymbol{\Omega}^{-1}\left[\frac{d^2\boldsymbol{y}_e^s}{d\lambda^2}(\lambda(t-\sigma))\left(\frac{d\lambda}{dt}(t-\sigma)\right)^2 + \frac{d\boldsymbol{y}_e^s}{d\lambda}(\lambda(t-\sigma)\frac{d^2\lambda}{dt^2}(t-\sigma)\right]d\sigma. \tag{3.16}$$

In summary, we have identified that trajectories track the quasi-static attractor with linear instantaneous lag $\boldsymbol{\ell}(t)$ and linear error $\boldsymbol{\epsilon}(t)$. The linear instantaneous lag is a linear approximation for how trajectories behave near the quasi-static attractor. Together with the linear error term, this tells us the complete non-linear dynamics of trajectories near the quasi-static attractor.

3.3 The Stable Region

3.3.1 Steady Drift Analysis

Provided that $\boldsymbol{\xi}$ is not time-dependent, we say that the system exhibits a **steady quasi-static drift**, **steady drift** or uniform parameter shift. Since the time derivative of a steady drift is zero, it follows that the system has a linear error of zero. In other words, (3.11) reduces to

$$\boldsymbol{y}(t) - \boldsymbol{y}_e^s(\lambda(t)) = \boldsymbol{\Omega}^{-1}\boldsymbol{\xi}. \tag{3.17}$$

If we take the vector norm [18, p. 552] of both sides, we obtain

$$\left|\left|\boldsymbol{y}(t) - \boldsymbol{y}_e^s(\lambda(t))\right|\right| = \left|\left|\boldsymbol{\Omega}^{-1}\boldsymbol{\xi}\right|\right|, \tag{3.18}$$

which tells us that we can avoid rate-dependent tipping if $\left|\left|\boldsymbol{\Omega}^{-1}\boldsymbol{\xi}\right|\right| < r$, for some arbitrary tipping radius $r > 0$. It turns out we can improve our criteria to avoid rate-dependent tipping

by manipulating matrix norms [18, p. 556]. If we define the subordinate matrix norm as

$$||\boldsymbol{\Omega}|| = \max_{\boldsymbol{w}\neq\boldsymbol{0}} \frac{||\boldsymbol{\Omega w}||}{||\boldsymbol{w}||}, \tag{3.19}$$

then we can make use of the following:

Proposition. $\forall \boldsymbol{\xi} \neq \boldsymbol{0}$ *and non-singular matrices* $\boldsymbol{\Omega}$*,*

$$||\boldsymbol{\Omega}||^{-1} \cdot ||\boldsymbol{\xi}|| \leq ||\boldsymbol{\Omega}^{-1}\boldsymbol{\xi}|| \leq ||\boldsymbol{\Omega}^{-1}|| \cdot ||\boldsymbol{\xi}||. \tag{3.20}$$

Proof. It follows from (3.19) that

$$||\boldsymbol{\Omega}^{-1}|| = \max_{\boldsymbol{\xi}\neq\boldsymbol{0}} \frac{||\boldsymbol{\Omega}^{-1}\boldsymbol{\xi}||}{||\boldsymbol{\xi}||} \geq \frac{||\boldsymbol{\Omega}^{-1}\boldsymbol{\xi}||}{||\boldsymbol{\xi}||} \iff ||\boldsymbol{\Omega}^{-1}\boldsymbol{\xi}|| \leq ||\boldsymbol{\Omega}^{-1}|| \cdot ||\boldsymbol{\xi}||.$$

As a consequence of the sub-multiplicative property [18, p. 559, (4)],

$$||\mathbb{I}|| = ||\boldsymbol{\Omega}\boldsymbol{\Omega}^{-1}|| \leq ||\boldsymbol{\Omega}|| \cdot ||\boldsymbol{\Omega}^{-1}||,$$

where $\mathbb{I}$ denotes the $n \times n$ identity matrix. Thus, it is clear that

$$||\boldsymbol{\xi}|| = ||\mathbb{I}\boldsymbol{\xi}|| = ||\boldsymbol{\Omega}\boldsymbol{\Omega}^{-1}\boldsymbol{\xi}|| \leq ||\boldsymbol{\Omega}|| \cdot ||\boldsymbol{\Omega}^{-1}\boldsymbol{\xi}|| \iff ||\boldsymbol{\Omega}||^{-1} \cdot ||\boldsymbol{\xi}|| \leq ||\boldsymbol{\Omega}^{-1}\boldsymbol{\xi}||.$$

□

Using this proposition, we can see that to avoid rate-dependent tipping, we require that

$$||\boldsymbol{\Omega}^{-1}|| \cdot ||\boldsymbol{\xi}|| < r, \tag{3.21}$$

and to induce rate-dependent tipping, we must have

$$||\boldsymbol{\Omega}||^{-1} \cdot ||\boldsymbol{\xi}|| > r. \tag{3.22}$$

3.3.2 Unsteady Drift Analysis

If we now assume that $\boldsymbol{\xi}$ depends on time, that is the system has unsteady drift, then by making use of the inequality

$$||e^{\boldsymbol{\Omega}\sigma}\boldsymbol{w}|| \leq ||e^{\boldsymbol{\Omega}\sigma}|| \cdot ||\boldsymbol{w}||, \tag{3.23}$$

we can derive the upper bound

$$||\boldsymbol{y}(t) - \boldsymbol{y}_e^s(\lambda(t))|| = \left|\left| \int_0^\infty e^{\boldsymbol{\Omega}\sigma} \frac{d\boldsymbol{y}_e^s}{dt} d\sigma \right|\right| \leq \int_0^\infty ||e^{\boldsymbol{\Omega}\sigma}|| \cdot \left|\left| \frac{d\boldsymbol{y}_e^s}{dt}(\lambda(t-\sigma)) \right|\right| d\sigma. \tag{3.24}$$

To simplify this result, we define the maximum quasi-static drift

$$\xi_{\max}(t) = \max_{t_0 \leq \tau \leq t} \left|\left| \frac{d\boldsymbol{y}_e^s}{dt}(\lambda(\tau)) \right|\right| = \max_{t_0 \leq \tau \leq t} \left|\left| \frac{d\boldsymbol{y}_e^s}{d\lambda}(\lambda(\tau)) \frac{d\lambda}{dt}(\lambda(\tau)) \right|\right|. \tag{3.25}$$

Using (3.25), we can rewrite the upper bound as

$$||\boldsymbol{y}(t) - \boldsymbol{y}_e^s(\lambda(t))|| \leq \xi_{\max}(t) \int_0^\infty ||e^{\boldsymbol{\Omega}\sigma}|| d\sigma. \tag{3.26}$$

We can also use that if $\boldsymbol{\Omega}$ is a stable matrix, then

$$||e^{\boldsymbol{\Omega}\sigma}|| \leq \alpha e^{-\beta\sigma}, \tag{3.27}$$

for $\alpha, \beta > 0$ [10, p. 263–264], to express the upper bound as

$$||\boldsymbol{y}(t) - \boldsymbol{y}_e^s(\lambda(t))|| \leq \xi_{\max}(t) \int_0^\infty \alpha e^{-\beta\sigma} d\sigma = \frac{\alpha}{\beta} \xi_{\max}(t). \tag{3.28}$$

From this, it is clear that to prevent rate-dependent tipping, we need to satisfy

$$\frac{\alpha}{\beta} \xi_{\max}(t) < r. \tag{3.29}$$

If we choose $\mathbf{\Omega} = -a^2$, where $a \in \mathbb{R}$, then $\left|\left|e^{\mathbf{\Omega}\sigma}\right|\right| = \left|e^{-a^2\sigma}\right|$, then we can rewrite (3.29) as

$$\frac{1}{a^2}\xi_{\max}(t) = \left|b^{-1}\right|\xi_{\max}(t) < r, \tag{3.30}$$

for $b = a^2$. This is reminiscent of condition (3.21), which is required to avoid rate-dependent tipping when dealing with steady drift. If we instead take $\mathbf{\Omega}$ to be a matrix, then optimising the tipping condition (3.29) become difficult. This is because knowledge of the structure of the matrix $\mathbf{\Omega}$ is required to choose suitable values for α and β. Therefore, it appears that for unsteady drift, it is difficult to find an optimal condition for rate-dependent tipping involving the maximum quasi-static drift using the tipping radius approach.

Remark. *Using the analysis we have done so far, we can estimate how long it takes for rate-dependent tipping to occur. A natural time-scale for the motion of the quasi-static attractor can be defined as*

$$\frac{r}{\left|\left|\boldsymbol{\xi}(t)\right|\right|} = r\left|\left|\frac{d\boldsymbol{y}_e^s}{d\lambda}\frac{d\lambda}{dt}\right|\right|^{-1}. \tag{3.31}$$

To convince ourselves this is an appropriate measure for time, we can find the dimensions for this quantity by making a dimensional analysis:

$$\left[\frac{r}{\left|\left|\boldsymbol{\xi}(t)\right|\right|}\right] = L\left(\frac{L}{T}\right)^{-1} = T, \tag{3.32}$$

where L is used to represent length and T is used to represent time. From our dimensional analysis, we can see that our time-scale has units of time, which is what we expect from a time-scale. Using this time-scale, we see that [2, p. 1172]:

- *if $r \approx 1$ and $\boldsymbol{y}_e^{s\prime}(\lambda) \approx 1$, then we expect tipping to occur when $\left|\lambda'(t)\right| \approx \left|\left|\mathbf{\Omega}\right|\right|$,*
- *if $r \approx 1$ and $\boldsymbol{y}_e^{s\prime}(\lambda) \approx 1/\varepsilon$ for some $0 < \varepsilon \ll 1$, then we expect tipping to occur when $\left|\lambda'(t)\right| \approx \varepsilon\left|\left|\mathbf{\Omega}\right|\right|$.*

Note that $\lambda'(t)$ means the derivative of λ with respect to t and $\boldsymbol{y}_e^{s\prime}(\lambda)$ means the derivative of $\boldsymbol{y}_e^s$ with respect to λ.

4 R-Tipping in a Saddle-Node Normal Form

So far, the phenomenon of rate-dependent tipping has been considered from a relatively abstract point of view. To get a different perspective of the material, we will now look at various examples to motivate the concept. The aim of this section and the next section is to analyse rate-dependent tipping in the bifurcation models we introduced in section 2. We start by considering the non-autonomous system

$$\frac{dx}{dt} = (x+\lambda)^2 - \mu, \quad \frac{d\lambda}{dt} = \xi, \tag{4.1}$$

where $x(t), \lambda(t) \in \mathbb{R}$, ξ is a steady drift and μ is a positive constant[3] [2, p. 9].

4.1 Analysis of a Saddle-Node Normal Form for Fixed λ

For fixed λ, we have $\dot{\lambda} = \xi = 0$, so the system becomes autonomous and has equilibrium points given by $\dot{x} = 0$. Thus, solving $\dot{x} = 0$ for x yields the lines of equilibria

$$x_e(\lambda)_\pm = -\lambda \pm \sqrt{\mu}. \tag{4.2}$$

If we set $\dot{x} = g(x)$, then we know from section 2 that the sign of $g'(x)$ evaluated at an equilibrium point tells us the stability of that equilibrium point. Clearly,

$$g'(x) = 2(x+\lambda), \tag{4.3}$$

and so it follows that

$$g'(x_e(\lambda)_\pm) = \pm 2\sqrt{\mu}. \tag{4.4}$$

Therefore, since $g'(x_e(\lambda)_-) < 0$, the line of equilibria defined by $x_e(\lambda)_-$ is stable. Similarly, since $g'(x_e(\lambda)_+) > 0$, the line of equilibria defined by $x_e(\lambda)_+$ is unstable. So in summary, the

[3] This is a saddle-node normal form with steady drift.

system has stable equilibrium

$$x_e^s(\lambda) = x_e(\lambda)_- = -\lambda - \sqrt{\mu} \tag{4.5}$$

and unstable equilibrium

$$x_e^u(\lambda) = x_e(\lambda)_+ = -\lambda + \sqrt{\mu}. \tag{4.6}$$

Thus, provided λ is taken to be fixed, trajectories in phase space converge to the stable equilibrium within the basin of attraction

$$\mathcal{R}^s = \left\{(x, \lambda) \in \mathbb{R}^2 : x < -\lambda + \sqrt{\mu}\right\}, \tag{4.7}$$

whilst trajectories in the region

$$\mathcal{R}^u = \left\{(x, \lambda) \in \mathbb{R}^2 : x > -\lambda + \sqrt{\mu}\right\} \tag{4.8}$$

are unbounded and diverge to infinity as $t \to \infty$. To take this analysis one step further, we can actually identify the nature associated with these stabilities. By inspection, we notice that there is a saddle-node bifurcation at $\mu = 0$. As a consequence of this, the stable equilibrium must be a stable node and the unstable equilibrium must be a saddle [21, p. 62, 63].

4.2 Steady Drift Analysis

For time dependent λ, the system has quasi-static attractor $x_e^s(\lambda(t))$ and quasi-static repeller $x_e^u(\lambda(t))$. It follows that the quasi-static attractor is a stable node and the quasi-static repeller is a saddle. Since the quasi-static equilibria vary in time, trajectories may no longer converge to the stable line. Instead, trajectories will roughly approach or track the quasi-static attractor. This is clearly an approximation for how the system behaves, but is enough to identify if the system tips or not. For instance, if trajectories fail to track the quasi-static attractor due to it varying in time too quickly, then the system has tipped as a

result of rate-dependent tipping. The rate at which the quasi-static equilibria move depends on the steady drift, ξ. So we are interested in identifying the values of ξ for which the system tips as a result of rate-dependent tipping.

4.2.1 Transforming to a Co–Moving Coordinate System

We can find the critical threshold, ξ_c, for the system by transforming to a **co-moving coordinate system**. Consider the transformation $\eta(t) = x(t) + \lambda(t)$. Applying this transformation to the original system yields the co-moving coordinate system

$$\frac{d\eta}{dt} = \eta^2 - \mu + \xi. \tag{4.9}$$

Notice how (4.9) does not depend on $\lambda(t)$. So transforming the original system to a co-moving coordinate system eliminates the systems dependence on $\lambda(t)$. As a consequence of this, our new system is an autonomous differential equation, and so has equilibrium points given by solutions to the equation $\dot{\eta} = 0$. The equilibrium points in the co-moving coordinate system tell us the exact behaviour of the original system. Since we only care about preventing the original system from tipping, we do not necessarily need to know the exact behaviour of the original system. Instead, we only need to know when trajectories fail to track the the quasi-static attractor in the original system.

If there is a stable equilibrium point in the co-moving coordinate system, then this transforms to a stable solution in the original system, which trajectories will converge to if they are within the stable solutions basin of attraction. This behaviour can be approximated by the quasi-static attractor. In other words, a stable equilibrium point in the co-moving coordinate system is equivalent to trajectories tracking the quasi-static attractor in the original system. If the stable equilibrium point destabilises in the co-moving system, then trajectories fail to track the quasi-static attractor in the original system. This destabilisation occurs when $\xi > \xi_c$. So analysing when the stable equilibrium point in the co-moving coordinate system destabilises tells us the value of the critical threshold ξ_c.

The equilibrium points in the co-moving coordinate system are given by

$$\eta_{e\pm} = \pm\sqrt{\mu - \xi}. \tag{4.10}$$

So there are two equilibrium points provided that $\xi < \mu$. In this case, we can find the stability of these equilibrium points by setting $\dot{\eta} = g(\eta)$. If we do this, then we find that

$$g'(\eta) = 2\eta, \tag{4.11}$$

which means we have

$$g'(\eta_{e\pm}) = \pm 2\sqrt{\mu - \xi}. \tag{4.12}$$

From this, we can deduce that η_{e-} is stable since $g'(\eta_{e-}) < 0$ and η_{e+} is unstable since $g'(\eta_{e+}) > 0$.

4.2.2 Original System Analysis

From our co-moving coordinate system analysis, it follows that in our original coordinate system, there are invariant lines defined by

$$x(\lambda(t))_{\pm} = -\lambda(t) \pm \sqrt{\mu - \xi}, \tag{4.13}$$

where the invariant line $x(\lambda(t))_-$ attracts trajectories and the invariant line $x(\lambda(t))_+$ repels trajectories. Notice that when $\xi = 0$ i.e. when λ is taken to be constant, these reduce to the solutions for the time-independent parameter system. So these invariant lines are simply translations of the quasi-static equilibria in the original system.

To identify the critical threshold ξ_c, we need to consider how the system behaves for different values of ξ:

- If $0 < \xi < \mu$, then $x(\lambda(t))_- = x^s(\lambda(t))$ and $x(\lambda(t))_+ = x^u(\lambda(t))$ are stable and unstable respectively. So for a steady drift in this range, trajectories track the quasi–static

attractor within the basin of attraction

$$\tilde{\mathcal{R}}^s = \{(x, \lambda) \in \mathbb{R}^2 : x < -\lambda + \sqrt{\mu - \xi}\} \tag{4.14}$$

and trajectories in the region

$$\tilde{\mathcal{R}}^u = \{(x, \lambda) \in \mathbb{R}^2 : x > -\lambda + \sqrt{\mu - \xi}\} \tag{4.15}$$

diverge to infinity as $t \to \infty$. Because of this change in behaviour depending on what side of the line $x^u(\lambda(t))$ trajectories are on, we say that the unstable invariant line defines a **tipping threshold**.

- If $\xi = \mu$, then geometrically the invariant lines coalesce to form a single invariant line, $x(\lambda(t))$. To identify the stability of this line, we can make use of the fact that $\mu = \xi$ is a saddle-node bifurcation, so a sketch of the bifurcation diagram, as illustrated in figure 4.1, reveals the line to be half-stable or **neutrally stable** [2, p. 9].

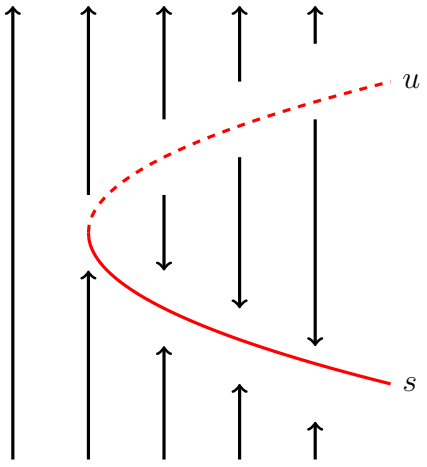

Figure 4.1: The bifurcation diagram for the co-moving coordinate system.

- If $\xi > \mu$, then there are no real solutions. This can be interpreted as the lines being destroyed as they pass one another. Since there are no longer stable or unstable regions

in the phase space, trajectories are unbounded for all initial conditions as $t \to \infty$. In other words, trajectories no longer track the quasi-static attractor.

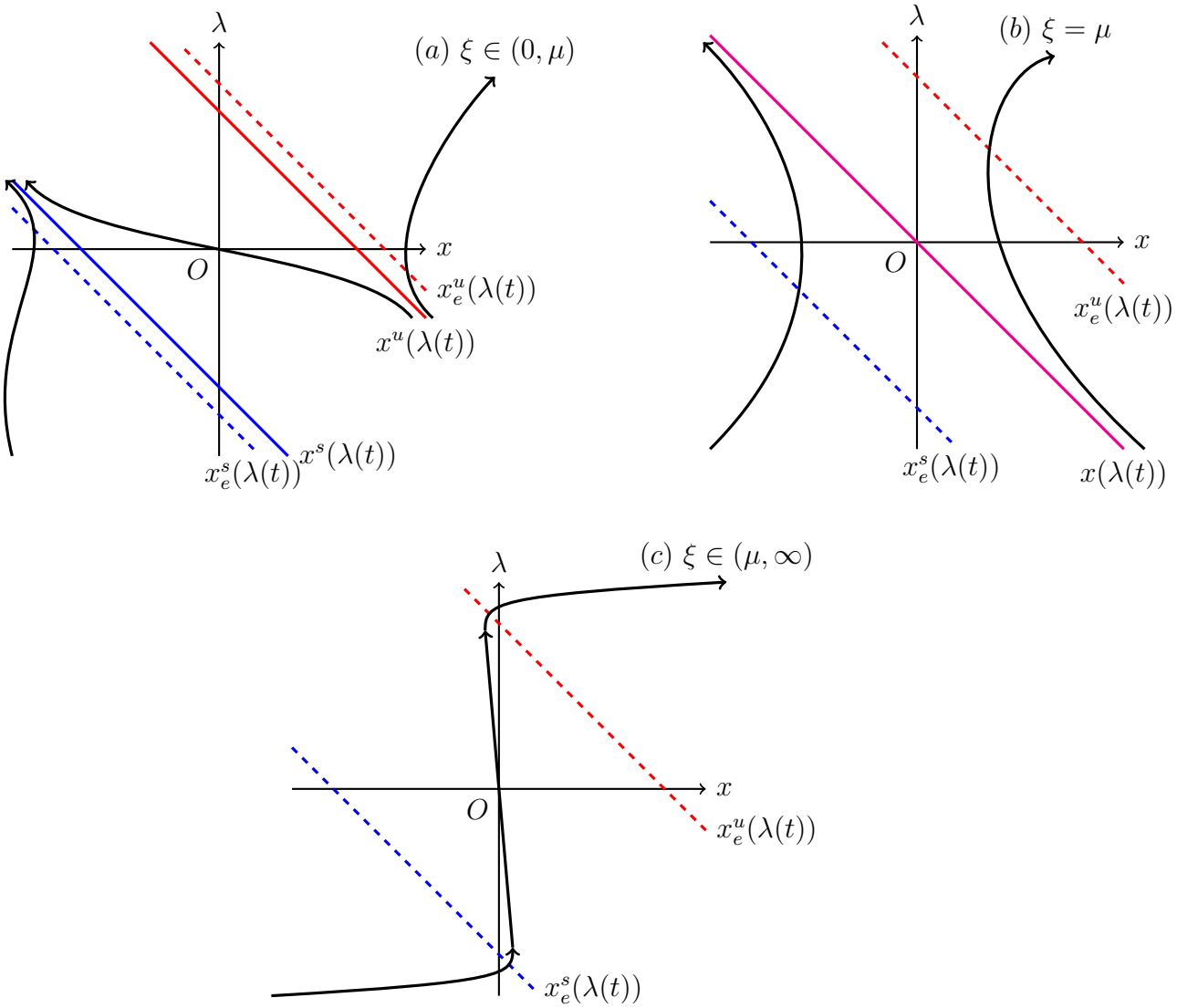

Figure 4.2: Phase portraits for (4.1) given different values of steady drift. This includes when: (a) $\xi \in (0, \mu)$, (b) $\xi = \mu$ and (c) $\xi \in (\mu, \infty)$.

4.2.3 Deriving the Critical Threshold

With these observations, we can now derive the critical threshold ξ_c. That is, we can formulate the steady drift for which the system destabilises if exceeded. Suppose we restrict initial

conditions, (x_0, λ_0), to the region

$$\{(x, \lambda) \in \mathbb{R}^2 : -\lambda < x < -\lambda + \sqrt{\mu}\}.$$

Then, the critical threshold is the value of ξ for which the tipping threshold $x^u(\lambda(t))$ intersects the point (x_0, λ_0). In this case we have initial conditions below the line $x = -\lambda$, trajectories will track the quasi-static attractor since $(x_0, \lambda_0) \in \tilde{\mathcal{R}}^s$ (provided the invariant lines have not yet coalesced). When the invariant lines coalesce, the tipping threshold vanishes. Since the lines meet before the tipping threshold enters the region $x < -\lambda$, we can deduce that the critical threshold must be the value of ξ for which the invariant lines vanish and leave trajectories unbounded as $t \to \infty$. In summary, the system tips for $\xi > \xi_c$, where

$$\xi_c(\mu) = \begin{cases} \mu - (x_0 + \lambda_0)^2 & \text{if } -\lambda_0 < x_0 < -\lambda_0 + \sqrt{\mu}, \\ \mu & \text{if } x_0 \leq -\lambda_0. \end{cases} \tag{4.16}$$

Remark. *Since $\lambda(t)$ is the function which causes the system to tip, it might be more convenient to express the inequalities defining the critical threshold in terms of λ_0 rather than x_0. This is easily done since the regions defining the critical threshold are straight lines, so the inequalities can be rearranged nicely.*

4.3 Tipping Radius Analysis for Steady Drift

Alternatively, we could have adopted a tipping radius approach to this problem to approximate the critical threshold. Recall the criteria for rate-dependent tipping with steady drift we derived for the linear model (3.3). Since we can linearise about the quasi-static attractor to get the linear equation

$$\frac{dx_1}{dt} = -2\sqrt{\mu}x_1, \tag{4.17}$$

where x_1 is a small perturbation in x, we can compare our linearisation with our linear model

for tipping radius. This reveals that we can approximate the critical threshold for the system by taking $\mathbf{\Omega} = -2\sqrt{\mu}$. If we do this, it follows that

$$\left|\left|\mathbf{\Omega}^{-1}\right|\right| = \left|\left|\mathbf{\Omega}\right|\right|^{-1} = (2\sqrt{\mu})^{-1} = \frac{1}{2\sqrt{\mu}}, \tag{4.18}$$

so this approximation tells us that the system does not tip as long as

$$\frac{\left|\xi_c\right|}{2\sqrt{\mu}} < r. \tag{4.19}$$

From the phase portraits for the linearised system, we can see geometrically that the linearised system tips when r is greater than the distance between the quasi-static attractor and its basin boundary i.e. the quasi-static repeller. This suggests the tipping radius to be

$$r = \left|x_e^s(\lambda(t)) - x_e^u(\lambda(t))\right| = \left| -\lambda - \sqrt{\mu} - (-\lambda + \sqrt{\mu})\right| = 2\sqrt{\mu}. \tag{4.20}$$

However, comparing this with (4.19) overestimates the critical threshold as $\xi_c = 4\mu$.

We know from our earlier analysis what the true value of the critical threshold is. Thus, we can find an **effective tipping radius** which will be 'effective' in obtaining the true value of the critical threshold. If we introduce an effective tipping radius $\Re$, then it follows from (3.21) that the system does not exhibit rate-dependent tipping provided that

$$\frac{\left|\xi_c\right|}{2\sqrt{\mu}} < \Re \iff \left|\xi_c\right| < 2\Re\sqrt{\mu}. \tag{4.21}$$

Comparing (4.21) with (4.16), when $\xi_c = \mu$, our tipping radius analysis suggests that an effective tipping radius is $\Re = 1/2\sqrt{\mu}$. Therefore, the linearised system must be a distance of $1/2\sqrt{\mu}$ away from the quasi-static attractor in order for the non-linear system to tip.

5 R-Tipping in a Subcritical Hopf Normal Form

In this section, we will analyse rate-dependent tipping in a different bifurcation model to that considered in section 4, namely the subcritical Hopf normal form. As we did with the saddle-node normal form, the aim of this section is to identify the critical threshold which forces the system to tip as a result of rate-dependent tipping.

5.1 Analysis of a Subcritical Hopf Normal Form for Fixed λ

We shall now concern ourselves with models which take the form

$$\frac{dz}{dt} = F(z - \lambda), \tag{5.1}$$

where $z \in \mathbb{C}$ and

$$F(z) = (-1 + i\omega)z + \left|z\right|^2 z \tag{5.2}$$

for some angular frequency ω[4].

If we take λ to be constant, then the system has equilibrium points given by $\dot{z}_e = 0$, that is

$$\begin{aligned} 0 &= \big(z_e - \lambda\big)\big(-1 + i\omega + \left|z_e - \lambda\right|^2\big) \\ \implies \quad z_e &= \lambda \ \text{ or } \ i\omega = 1 - \left|z_e - \lambda\right|^2. \end{aligned} \tag{5.3}$$

Since $\left|z_e - \lambda\right|^2 \in \mathbb{R}$, it is clear that for non-zero angular frequency, the system has a single equilibrium point, $z_e(\lambda) = \lambda$. To identify the stability of $z_e(\lambda) = \lambda$, we must find the Jacobian matrix for the system. We can do this by expressing the complex differential equation as a system of two real differential equations. If we set $z(t) = x(t) + iy(t)$, where $x(t), y(t) \in \mathbb{R}$,

[4] This is a subcritical Hopf normal form.

then by equating real and imaginary parts, we obtain the system

$$\begin{aligned}\frac{dx}{dt} &= (x-\lambda)\big[-1+(x-\lambda)^2+y^2\big]-\omega y,\\ \frac{dy}{dt} &= y\big[-1+(x-\lambda)^2+y^2\big]+\omega(x-\lambda).\end{aligned} \tag{5.4}$$

This system has Jacobian matrix given by

$$\boldsymbol{J}(x,y)=\begin{bmatrix} -1+3(x-\lambda)^2+y^2 & 2(x-\lambda)y-\omega \\ 2(x-\lambda)y+\omega & -1+3y^2+(x-\lambda)^2 \end{bmatrix}, \tag{5.5}$$

which evaluated at $z_e(\lambda)=\lambda$, becomes

$$\boldsymbol{J}(\lambda,0)=\begin{bmatrix} -1 & -\omega \\ \omega & -1 \end{bmatrix}. \tag{5.6}$$

One can find the eigenvalues of this matrix to be $\gamma_\pm=-1\pm i\omega$, so we can conclude that the system, for constant λ, has stable spiral, $z_e^s(\lambda)=\lambda$.

Our analysis so far only takes into account when the system has non-zero angular frequency. It turns out that when $\omega=0$, the system has periodic orbit, $\big|z_e-\lambda\big|=1$. In Cartesian form, this becomes $(x_e-\lambda)^2+y_e^2=1$, which has the corresponding Jacobian matrix

$$\boldsymbol{J}(x_e,y_e)=\begin{bmatrix} 2(x_e-\lambda)^2 & 2(x_e-\lambda)y_e \\ 2(x_e-\lambda)y_e & 2y_e^2 \end{bmatrix}. \tag{5.7}$$

The trace of this matrix is

$$\operatorname{tr}\boldsymbol{J}(x_e,y_e)=2(x_e-\lambda)^2+2y_e^2=2>0, \tag{5.8}$$

which tells us that the periodic orbit is unstable. In other words, the stable equilibrium

$z_e^s(\lambda) = \lambda$ has basin of attraction, in Cartesian form, defined by

$$\mathcal{R} = \{(x, y, \lambda) \in \mathbb{R}^3 : (x - \lambda)^2 + y^2 < 1\}. \tag{5.9}$$

5.2 Steady Drift Analysis

Now suppose that λ is time-dependent. In this case, the system has the quasi-static attractor $z_e^s(\lambda(t)) = \lambda(t)$. Suppose that the system shifts along the real axis with positive steady drift $\dot{\lambda} = \xi > 0$. Similar to what we saw with the saddle-node normal form, we will see later that there is a critical threshold, ξ_c, such that when $\xi > \xi_c$, trajectories for the system diverge from the quasi-static attractor. Our aim is to find an analytic form for this rate.

5.2.1 Transforming to a Co-Moving Coordinate System

We can calculate such a rate by transforming the system to the co-moving coordinate system defined by $\eta(t) = z(t) - \lambda(t) \in \mathbb{C}$. As a consequence of the chain rule, we have

$$\frac{dz}{dt} = \frac{\partial z}{\partial \eta}\frac{d\eta}{dt} + \frac{\partial z}{\partial \lambda}\frac{d\lambda}{dt} = \frac{d\eta}{dt} + \xi, \tag{5.10}$$

so it is clear that this transformation gives us the system

$$\frac{d\eta}{dt} = F(\eta) - \xi = (-1 + i\omega)\eta + \left|\eta\right|^2\eta - \xi. \tag{5.11}$$

For $\xi = 0$, that is when λ is constant, $\eta = 0$ satisfies the differential equation. We expect this since for fixed λ, the original system has the equilibrium point $z_e^s(\lambda) = \lambda$, so our transformation gives us $\eta_e = z_e - \lambda = 0$. Therefore, this equation tells us that when $\xi = 0$, the transformed quasi-static attractor $\eta_e^s(\lambda) = 0$ is an equilibrium point of equation (5.11).

As a consequence of the co-moving coordinate transformation, we have eliminated the systems dependence on $\lambda(t)$. In other words, (5.11) is an autonomous differential equation, and so has equilibrium points given by solutions to the equation $\dot{\eta}_e = 0$. As with the

saddle-node normal form with steady drift, a stable equilibrium point in the co-moving coordinate system is equivalent to trajectories tracking the quasi-static attractor in the original system. So if a stable equilibrium point destabilises, then the original system no longer tracks the quasi-static attractor. When $\xi > \xi_c$, the stable equilibrium destabilises, and so the original system tips as a result of rate-dependent tipping. Thus, analysing when the stable equilibrium point in the co-moving coordinate system destabilises reveals the value of the critical threshold, ξ_c.

Since $\eta \in \mathbb{C}$, we can express it in polar form as $\eta = |\eta|e^{i\theta}$, so we can rewrite the right-hand side of (5.11) as

$$F(|\eta|e^{i\theta}) - \xi = |\eta|e^{i\theta}(-1 + i\omega + |\eta|^2) - \xi. \tag{5.12}$$

It follows that equilibrium points, $(|\eta_e|, \theta_e)$, in this system must satisfy

$$\begin{aligned} & |\eta_e|e^{i\theta_e}(-1 + i\omega + |\eta_e|^2) - \xi = 0 \\ \implies & \left||\eta_e|e^{i\theta_e}(-1 + i\omega + |\eta_e|^2)\right|^2 = |\xi|^2 \\ \implies & |\eta_e|^6 - 2|\eta_e|^4 + (1+\omega^2)|\eta_e|^2 = \xi^2. \end{aligned} \tag{5.13}$$

5.2.2 Analysing the Equilibrium Equation

Equation (5.13) can either be thought of as a polynomial of degree 6 in the variable $|\eta_e|$, or a cubic in the variable $|\eta_e|^2$. We shall refer to this equation from now on as the **equilibrium equation** for the system. In order to analyse the solutions to our equilibrium equation, let us define

$$h(y) := y^3 - 2y^2 + (1+\omega^2)y, \tag{5.14}$$

where $y = |\eta_e|^2$. By inspection, we notice that $y = 0$ is exactly a root of $h(y)$. This tells us that the other roots for the cubic equation can be found by solving

$$y^2 - 2y + 1 + \omega^2 = 0. \tag{5.15}$$

From this, it follows that the other two roots of the cubic equation are complex conjugates of the form $y(\omega)_{\pm} = 1 \pm i\omega$. Hence, the cubic equation defined by $h(y)$ crosses the y-axis at the origin only. If $y \to \pm\infty$, then $h(y) \to \pm\infty$ since for large values of y, $h(y) \approx y^3$. We can find the maximum and minimum points of $h(y)$ by solving

$$\frac{dh}{dy} = 3y^2 - 4y + 1 + \omega^2 = 0 \tag{5.16}$$

for y. Following this calculation through, we find that

$$y_S(\omega)_{\pm} = \frac{2}{3}\left[1 \pm \sqrt{1 - \frac{3}{4}(1+\omega^2)}\,\right], \tag{5.17}$$

where y_S is used to denote the values of y for which $h(y)$ has stationary values. Notice that there are only two stationary points provided that $1 - 3/4(1+\omega^2) > 0$. If $\omega^2 = 1/3$, then the stationary point is a point of inflection and if $\omega^2 > 1/3$, then there are no stationary points at all. So $h(y)$ has two stationary points for $0 < \omega^2 < 1/3$ (since ω^2 is strictly positive). Using this inequality, we see that $1/3 < y_S(\omega)_- < 2/3$ and $2/3 < y_S(\omega)_+ < 1$, so stationary points for $h(y)$ must lie in the region

$$\frac{1}{3} < y < 1. \tag{5.18}$$

Since $h(y)$ only crosses the y-axis at the origin, and we have shown that $h(y)$ is large and positive for large values of y, (5.18) tells us that the maximum and minimum values of $h(y)$ must be positive.

Now we can analyse the equilibrium points of the system. As a consequence of the equilibrium equation (5.13), the equilibrium points for the system are given by the points of intersection between the curve $h = h(y)$ and the line $h = \xi^2$. If we consider the case where $\omega^2 < 1/3$, then there are three possibilities for the types of intersection the line $h = \xi^2$ makes with $h = h(y)$:

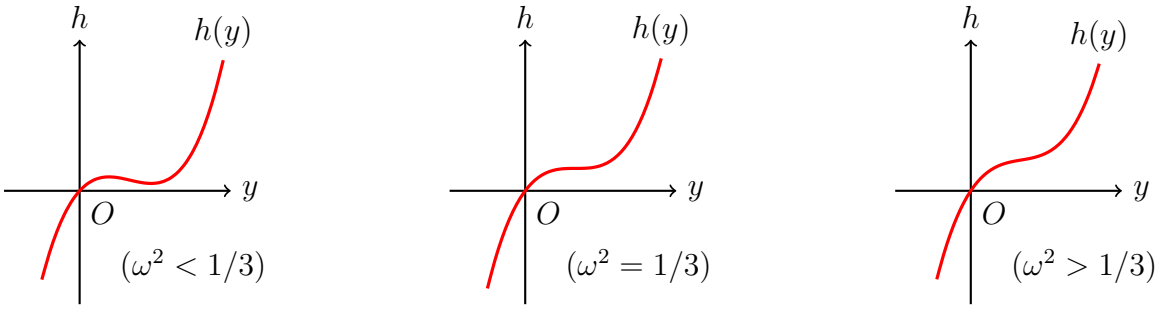

Figure 5.1: Sketches of $h(y)$ for $\omega^2 < 1/3$, $\omega^2 = 1/3$ and $\omega^2 > 1/3$.

- $h = \xi^2$ intersects $h = h(y)$ at three distinct points,
- $h = \xi^2$ is tangent to $h = h(y)$ at a stationary point,
- $h = \xi^2$ intersects $h = h(y)$ at a single point.

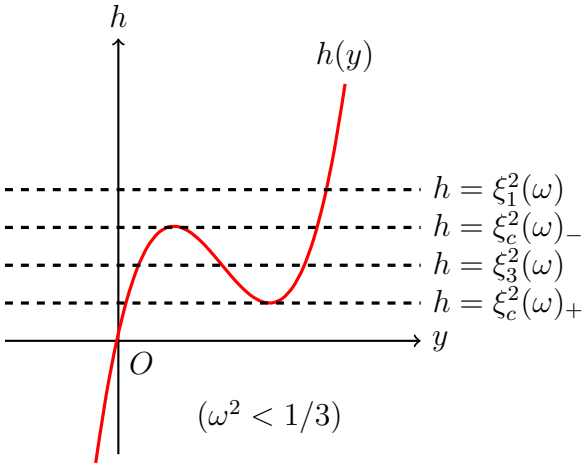

Figure 5.2: A sketch of the types of intersection the line $h = \xi^2$ can make with $h = h(y)$ when $\omega^2 < 1/3$.

It is clear from figure 5.2 that the number of equilibrium points changes from 3 to 1 as the line $h = \xi^2$ moves passed points of tangency. In other words, there are saddle-node bifurcations at the points where $h = \xi^2$ is tangent to the cubic $h = h(y)$, that is, when $\xi^2 = \xi_c^2(\omega)_\pm$. So

the system has saddle-node bifurcation curves defined by

$$\xi_c^2(\omega)_\pm = y_S^3(\omega)_\pm - 2y_S^2(\omega)_\pm + (1+\omega^2)y_S(\omega)_\pm. \tag{5.19}$$

Along these curves there are saddle-node bifurcations. So as we cross these curves, the number of equilibria changes from 3 to 1 as a result of 2 equilibria disappearing in a saddle-node bifurcation. There are two saddle-node bifurcation curves provided that

$$1 - \frac{3}{4}(1+\omega^2) > 0. \tag{5.20}$$

In the case this inequality does not hold, the curves disappear. The point at which these curves disappear is when the inequality (5.20) becomes an equality, that is, when $\omega^2 = 1/3$. Hence, in the parameter space defined by (ω, ξ), the branches for the saddle-node bifurcation curves join together tangentially at the **cusps points** $(\omega_\pm, \xi) = (\pm(1/3)^{1/2}, (2/3)^{3/2}\ )$ and vanish.

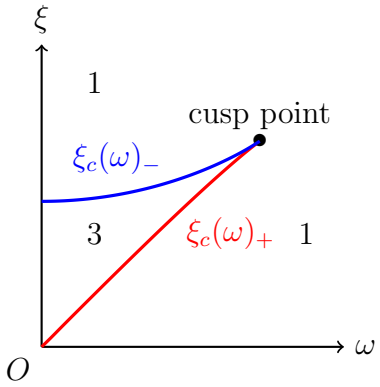

Figure 5.3: A plot of the saddle-node bifurcation curves in the positive quadrant of the parameter space defined by (ω, ξ).

We will call figure 5.3 and similar diagrams **stability diagrams**. Since the analytic forms for these curves are even functions, the complete saddle-node bifurcation curves are symmetric about the ξ-axis. Annotated on the diagram are the numbers 1 and 3. In the space between

the two saddle-node curves, the number 3 tells us that the system has 3 equilibrium points for parameter values in this region. If we cross these curves and move outside this region, then the number of equilibrium points changes from 3 to 1 due to two equilibria disappearing in a saddle-node bifurcation. Alternatively, we can plot our results in the form of a **cusp catastrophe surface** [22, p. 70-73] using MATLAB, as in figure 5.4.

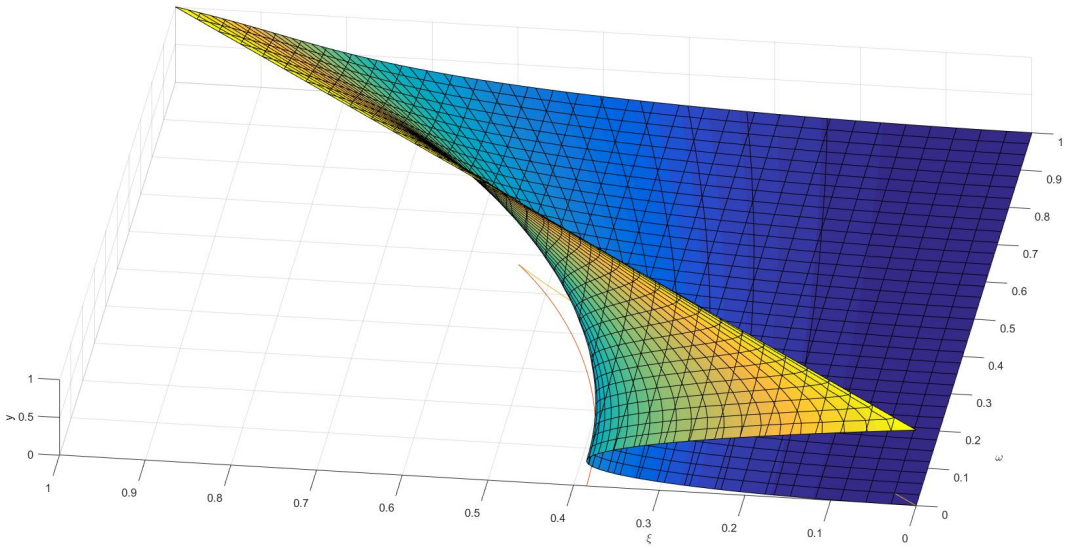

Figure 5.4: Cusp catastrophe surface for the co-moving coordinate system.

Note that in figure 5.4, below the surface in the (ω, ξ)-parameter plane are the saddle-node bifurcation curves. These are projections of the cusp catastrophe surface folding over on itself. Notice that beyond the cusp point, the cusp catastrophe surface no longer folds over on itself.

5.2.3 Stability Analysis

To analyse the behaviour of the co-moving coordinate system surrounding equilibrium points, we can rewrite the complex differential equation as a system of two real differential equations. Since the co-moving coordinate system is defined by $\eta = z - \lambda = (x - \lambda) - iy$, we can transform

(5.4) according to this to rewrite (5.11) as the system

$$\begin{aligned}\frac{d\tilde{x}}{dt} &= \tilde{x}(-1+\tilde{x}^2+\tilde{y}^2)-\omega\tilde{y}-\xi,\\ \frac{d\tilde{y}}{dt} &= \tilde{y}(-1+\tilde{x}^2+\tilde{y}^2)+\omega\tilde{x},\end{aligned} \tag{5.21}$$

where $\tilde{x} = x - \lambda$ and $\tilde{y} = y$ are the real and imaginary parts of η. From this, we find the Jacobian matrix to be

$$\boldsymbol{J}(\tilde{x},\tilde{y}) = \begin{bmatrix} -1+3\tilde{x}^2+\tilde{y}^2 & 2\tilde{x}\tilde{y}-\omega \\ 2\tilde{x}\tilde{y}+\omega & -1+\tilde{x}^2+2\tilde{y}^2 \end{bmatrix}. \tag{5.22}$$

Thus, evaluating (5.22) at the equilibrium point $\eta_e = \tilde{x}_e + i\tilde{y}_e$ gives us

$$\boldsymbol{J}(\tilde{x}_e,\tilde{y}_e) = \begin{bmatrix} -1+2\tilde{x}_e^2+\big|\eta_e\big|^2 & 2\tilde{x}_e\tilde{y}_e-\omega \\ 2\tilde{x}_e\tilde{y}_e+\omega & -1+2\tilde{y}^2+\big|\eta_e\big|^2 \end{bmatrix}, \tag{5.23}$$

where we have made use of the identity $\big|\eta_e\big|^2 = \tilde{x}_e^2 + \tilde{y}_e^2$. We can also use the identity $\big|\eta_e\big|^4 = \tilde{x}_e^4 + 2\tilde{x}_e^2\tilde{y}_e^2 + \tilde{y}_e^4$ to express the trace and determinant of $\boldsymbol{J}(\tilde{x}_e,\tilde{y}_e)$ as

$$\operatorname{tr}\boldsymbol{J}\big(\big|\eta_e\big|\big) = 2\big(2\big|\eta_e\big|^2-1\big), \quad \det\boldsymbol{J}\big(\big|\eta_e\big|\big) = 1+\omega^2-4\big|\eta_e\big|^2+3\big|\eta_e\big|^4. \tag{5.24}$$

If we factorise our expression for the determinant, we obtain the characteristic polynomial

$$\gamma^2 + 2\big(1-2\big|\eta_e\big|^2\big)\gamma + \omega^2 + \big(3\big|\eta_e\big|^2-1\big)\big(\big|\eta_e\big|^2-1\big) = 0. \tag{5.25}$$

From this, we see that the eigenvalues for the Jacobian matrix are

$$\gamma_\pm = 2\big|\eta_e\big|^2 - 1 \pm \sqrt{\big|\eta_e\big|^4-\omega^2}. \tag{5.26}$$

The equilibrium point, η_e, is stable, provided that

$$\operatorname{tr} \boldsymbol{J}\big(|\eta_e|\big) < 0 \quad \text{and} \quad \det \boldsymbol{J}\big(|\eta_e|\big) > 0. \tag{5.27}$$

As a consequence of the trace inequality, we must have $|\eta_e|^2 < 1/2$. Using this result, we can complete the square to show that

$$\det \boldsymbol{J}\big(|\eta_e|\big) = 3\left(\frac{2}{3} - |\eta_e|^2\right)^2 + \omega^2 - \frac{1}{3} > \omega^2 - \frac{1}{4}. \tag{5.28}$$

Therefore, it is clear from (5.28) that $\det \boldsymbol{J}\big(|\eta_e|\big) > 0$ as long as $\omega^2 > 1/4$. In other words:

- η_e is stable if $|\eta_e|^2 < 1/2$ and $\omega^2 > 1/4$,
- η_e is unstable if $|\eta_e|^2 > 1/2$ or $|\eta_e|^2 < 1/2$ and $\omega^2 < 1/4$.

5.2.4 Hopf Bifurcation Analysis

The system also has a Hopf bifurcation. Recall from section 2 that a Hopf bifurcation occurs when the eigenvalues associated with the equilibrium point are complex conjugates and cross the imaginary axis. When the eigenvalues meet the imaginary axis, they are purely imaginary. The system has purely imaginary complex conjugate eigenvalues when

$$2|\eta_e|^2 - 1 = 0 \quad \text{and} \quad |\eta_e|^4 - \omega^2 < 0. \tag{5.29}$$

Thus, the system has a Hopf bifurcation when $|\eta_e|^2 = 1/2$ and $\omega^2 > 1/4$. By substituting these results into our equilibrium equation for the system, we find that this bifurcation occurs when $\xi^2 > 1/4$. Once the eigenvalues cross the imaginary axis, they become complex conjugates again and not just purely imaginary. As such, the stability of the equilibrium point depends on the real component of the eigenvalues, that being the quantity $2|\eta_e|^2 - 1$. If $|\eta_e|^2 < 1/2$, then the equilibrium point is stable and if $|\eta_e|^2 > 1/2$, the equilibrium point is unstable (this is consistent with our earlier stability analysis for η_e).

Since there is a Hopf bifurcation when $\omega^2, \xi^2 > 1/4$ and $\left|\eta_e\right|^2 = 1/2$, in the parameter space the Hopf bifurcation curves originate from the points $(\omega_\pm, \xi) = (\pm 1/2, 1/2)$, where these curves are defined by

$$\xi(\omega) = \sqrt{\frac{1}{8}(1 + 4\omega^2)}, \quad \omega^2 > \frac{1}{4}. \tag{5.30}$$

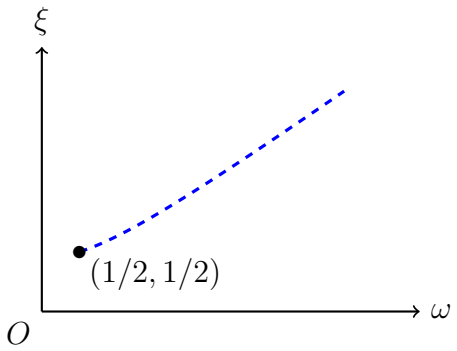

Figure 5.5: The Hopf bifurcation curve for $\omega > 0$. Since (5.30) is an even function, the complete stability diagram is symmetric about the ξ-axis.

So the system has two types of bifurcation, namely a saddle-node bifurcation and a Hopf bifurcation. This combination of bifurcations is called a **Bogdanov-Takens bifurcation**. Notice that if we substitute $\left|\eta_e\right|^2 = 1/2$ into our tangency condition for the saddle–node bifurcation, we obtain $\omega_\pm = \pm 1/2$. This means that the saddle-node bifurcation curves and the Hopf bifurcation curves in the parameter space meet at the points where the Hopf bifurcation curves originate. These points are called **Bogdanov-Takens bifurcation points**.

5.2.5 Distinguishing Saddle-Node Bifurcation Curves

Recall that a saddle-node bifurcation occurs when an eigenvalue passes through the origin along the real line (so that the system changes stability). In other words, one solution for

our characteristic polynomial (5.25) must be $\gamma = 0$. To verify this, substitution of $\gamma = 0$ into (5.25) yields

$$\omega^2 + \left(3\left|\eta_e\right|^2 - 1\right)\left(\left|\eta_e\right|^2 - 1\right) = 0, \tag{5.31}$$

which when solved for $\left|\eta_e\right|^2$, gives us (5.17), which is simply the tangency condition for the saddle–node bifurcation. Now that we know that $\gamma = 0$ is a root of the characteristic polynomial in the case of a saddle-node bifurcation, we can substitute (5.31) into (5.25) to obtain the second root of the characteristic polynomial. Following this calculation through,

$$\gamma^2 + 2\left(1 - 2\left|\eta_e\right|^2\right)\gamma = 0, \tag{5.32}$$

which tells us that $\gamma = 0$ or $\gamma = 2\left(2\left|\eta_e\right|^2 - 1\right) = 4\left|\eta_e\right|^2 - 2$. Because we are considering a saddle-node bifurcation, we can rewrite the non-zero eigenvalue as

$$\gamma_\pm = \frac{2}{3}\left[1 \pm 4\sqrt{1 - \frac{3}{4}(1+\omega^2)}\,\right], \tag{5.33}$$

using the tangency condition. When $\omega^2 < 1/4$, we have $\gamma_+ > 4/3$ and $\gamma_- < 0$. We will call the saddle-node bifurcation subcritical in the instance the non-zero eigenvalue is positive and supercritical if the non-zero eigenvalue is negative.

5.2.6 Summary of Steady Drift Analysis

From our analysis of the Hopf normal form with steady drift, we can conclude that the stable equilibrium point in the co-moving system:

- is destroyed in a supercritical saddle-node bifurcation when $\omega^2 < 1/4$,
- becomes unstable in a subcritical Hopf bifurcation when $\omega^2 > 1/4$.

For fixed ω, the value of ξ determines whether the stable equilibrium destabilises. When $\omega^2 < 1/4$ (before Bogdanov-Takens), we can see from figure 5.6 that when we increase ξ to

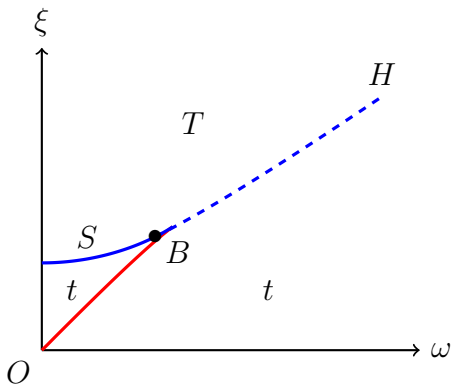

Figure 5.6: The complete stability diagram for positive ω and ξ, where: B represents the Bogdanov-Takens bifurcation point, H represents the subcritical Hopf bifurcation curve, S represents the supercritical saddle-node bifurcation curve, t represents the region where the system tracks the quasi-static attractor, and T represents the region where the system tips.

cross the subcritical saddle-node bifurcation curve, the number of equilibrium points changes from 1 to 3, so the stable equilibrium point does not destabilise. However, when we increase ξ to cross the supercritical saddle-node bifurcation curve, the stable equilibrium point is destroyed in a saddle-node bifurcation. For $\omega^2 > 1/4$ (after Bogdanov-Takens), the stable equilibrium becomes unstable in a subcritical Hopf bifurcation when we increase ξ to cross the subcritical Hopf bifurcation curve.

Recall that a stable equilibrium point destabilising in the co-moving coordinate system is equivalent to trajectories failing to track the quasi-static attractor when $\xi > \xi_c$. Hence, in summary, for initial conditions within the basin of attraction for the quasi-static attractor, we find the critical threshold to be

$$\xi_c(\omega) = \begin{cases} \sqrt{|\eta_e|_-^6 - 2|\eta_e|_-^4 + (1+\omega^2)|\eta_e|_-^2} & \text{if} \quad \omega^2 \leq 1/4, \\ \sqrt{\frac{1}{8}(1+4\omega^2)} & \text{if} \quad \omega^2 > 1/4. \end{cases} \tag{5.34}$$

5.3 Unsteady Drift Analysis

Up to this point, we have only considered analysis of systems with steady drift, that is we have only considered when ξ does not depend on time. We now turn our attention to unsteady drift and how this influences our subcritical Hopf normal form model.

Suppose that we model the movement of the quasi-static attractor with

$$\frac{d\lambda}{dt} = \rho\lambda(\alpha - \lambda), \quad \lambda(\tau) = \frac{1}{2}\alpha, \tag{5.35}$$

where $\rho > 0$, $\alpha > 0$ is the amplitude of the parameter shift and τ is the time when the rate of change of the quasi-static attractor is greatest. As a consequence of how we have defined τ, it follows that

$$\frac{d\lambda}{dt} \leq \frac{d\lambda}{dt}(\tau) = \frac{1}{4}\alpha^2\rho. \tag{5.36}$$

By making use of separation of variables, partial fractions and our boundary condition, we find that λ has the analytic form

$$\lambda(t) = \frac{\alpha e^{\alpha\rho(t-\tau)}}{e^{\alpha\rho(t-\tau)} + 1} = \frac{\alpha}{1 + e^{-\alpha\rho(t-\tau)}}, \tag{5.37}$$

which is in the form of logistic growth [16, p. 3]. It is clear from (5.37) that:

$$\lim_{t\to\infty} \lambda(-t) = 0 \quad \text{and} \quad \lim_{t\to\infty} \lambda(t) = \alpha.$$

From figure 5.7, we can see that the parameter variation is continuous between $\lambda(t) = 0$ and $\lambda(t) = \alpha$, where these are asymptotes . It is also evident that the parameter variation in $\lambda(t)$ dies down near these asymptotes. If we substitute these values of $\lambda(t)$ into $\dot{z} = 0$, as defined in (5.3), we can identify the region in which the quasi-static attractor is shifted. We find that $z_e^s(0) = 0$ and $z_e^s(\alpha) = \alpha$, and so we have defined a continuous shift of the quasi-static attractor from $z = 0$ to $z = \alpha$.

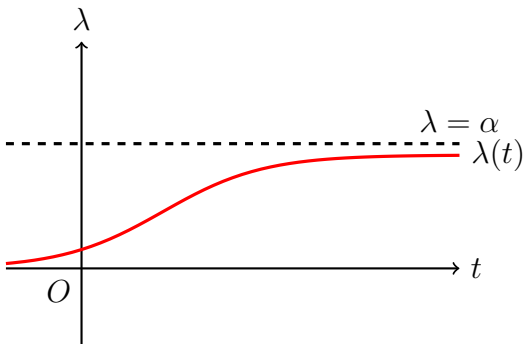

Figure 5.7: A graphical representation of (5.37).

For this parameter shift, there is no change in the stability of the quasi-static attractor. Moreover, it is clear from the quasi-static attractor having basin boundary

$$|z - \lambda| = 1, \tag{5.38}$$

that there is no change in the basin size. It turns out that the system has a critical threshold, ρ_c, such that when $\rho < \rho_c$, the system tracks the quasi-static attractor, and when $\rho > \rho_c$, then the system tips [2, p. 1176]. Since the rate of change for the motion of the quasi-static attractor dies down near the asymptotes $\lambda = 0$ and $\lambda = \alpha$, we can deduce that the system tips near $t = \tau$, as this is the region of time for which the parameter variation is most rapid. In the case of unsteady drift, we must rely on numerical methods to approximate the critical threshold, ρ_c [17, p. 100-102].

6 R-Tipping in a Fast-Slow System

The models we have considered up to this point have all involved locally stable equilibrium points. The purpose of this section is to demonstrate to the reader that a system can still exhibit rate-dependent tipping even where there is a single globally asymptotically stable equilibrium point.

Remark. *Throughout this section, we will be working with a pair of time scales, namely t and τ. When writing time derivatives using shorthand notation, we will use $\dot{x}$ to denote the derivative with respect to t and x' to denote the derivative with respect to τ.*

6.1 Introducing the Model

Our model of interest will be a fast-slow system which has a unique, globally stable quasi-static equilibrium in the neighbourhood of a locally folded critical slow manifold. Fast-slow systems arise in many applications, particularly in (but not limited to) mathematical biology when working with biological systems [11, 4]. A more specific, but complicated example of such a system is the compost-bomb instability [24, p. 1261-1265]. In our case, we shall study the simple fast-slow system[5]

$$\begin{aligned} \varepsilon\frac{dx}{dt} &= y + \lambda + x(x-1), \\ \frac{dy}{dt} &= -\sum_{n=1}^{2m+1} x^n, \end{aligned} \tag{6.1}$$

where $m \in \mathbb{N}$, $x \in \mathbb{R}$ is a fast variable, $y \in \mathbb{R}$ is a slow variable and $0 < \varepsilon \ll 1$ (the ratio between the time scales of the fast and slow variables). This system of equations is called the **slow system** since we have derivatives of the fast and slow variables with respect to the slow time scale t. We can express the system in terms of the fast time scale by making the change of variables $\tau = t/\varepsilon$, where τ is the fast time scale. It follows from the chain rule that

[5] Such systems are sometimes called **singularly perturbed systems** due to a differential equation being **singular** because of the presence of ε.

the system becomes

$$\begin{aligned} \frac{dx}{d\tau} &= y + \lambda + x(x-1), \\ \frac{dy}{d\tau} &= -\varepsilon \sum_{n=1}^{2m+1} x^n, \end{aligned} \quad . \tag{6.2}$$

We call this system of equations the **fast system**.

6.2 Analysing a Fast-Slow System for Fixed λ

6.2.1 Equilibrium Analysis

For fixed λ, the fast system has equilibrium points given by solutions to the equations $x_e' = 0$ and $y_e' = 0$. To solve $y_e' = 0$, we can rewrite the geometric sum as

$$\sum_{n=1}^{2m+1} x^n = \frac{x(1-x^{2m+1})}{1-x}, \tag{6.3}$$

for $x \neq 1$, which converges for $|x| < 1$ and diverges for $|x| \geq 1$ [19, p. 152]. From this, we see that

$$\frac{dy_e}{d\tau} = 0 \implies x_e = 0, \tag{6.4}$$

since $x \neq 1$, and

$$\frac{dx_e}{d\tau} = 0 \implies y_e = x_e(1-x_e) - \lambda = -\lambda, \tag{6.5}$$

so the fast system has the unique equilibrium point $\boldsymbol{x}_e(\lambda) = (0, -\lambda)$. By inspection of the fast system, we find the Jacobian matrix to be

$$\boldsymbol{J}(x,y) = \begin{bmatrix} 2x-1 & 1 \\ -\varepsilon \sum_{n=1}^{2m+1} n x^{n-1} & 0 \end{bmatrix}. \tag{6.6}$$

We can expand the summation inside the Jacobian matrix as

$$\sum_{n=1}^{2m+1} nx^{n-1} = \frac{d}{dx}\left[\frac{x(1-x^{2m+1})}{1-x}\right] = \frac{(2m+1)x^{2m+2} - (2m+2)x^{2m+1} + 1}{(1-x)^2}, \tag{6.7}$$

for $x \neq 1$. So it is clear that the Jacobian matrix evaluated at the equilibrium point is

$$\boldsymbol{J}(0, -\lambda) = \begin{bmatrix} -1 & 1 \\ -\varepsilon & 0 \end{bmatrix}. \tag{6.8}$$

From this, we see that

$$\operatorname{tr} \boldsymbol{J}(\boldsymbol{x}_e(\lambda)) = -1 < 0 \quad \text{and} \quad \det \boldsymbol{J}(\boldsymbol{x}_e(\lambda)) = \varepsilon > 0, \tag{6.9}$$

so $\boldsymbol{x}_e(\lambda)$ is a stable equilibrium point. In addition, we have that

$$\operatorname{tr}^2 \boldsymbol{J}(\boldsymbol{x}_e(\lambda)) - 4 \det \boldsymbol{J}(\boldsymbol{x}_e(\lambda)) = 2 - 4\varepsilon \approx 2 > 0, \tag{6.10}$$

since ε is a very small parameter. Thus, the equilibrium point, $\boldsymbol{x}_e(\lambda)$, is a stable node. In fact, it turns out that $\boldsymbol{x}_e(\lambda)$ is asymptotically stable for any fixed λ and globally asymptotically stable if $m \geq 2$ [2, 1177].

6.2.2 The Critical Manifold

Since ε is a very small parameter, we can approximate the dynamics of the system in the **singular limit** $\varepsilon \to 0$. Consideration of this limit for (6.1) and (6.2) yields the systems

$$\begin{aligned} 0 &= y + \lambda + x(x-1), \\ \frac{dy}{dt} &= -\sum_{n=1}^{2m+1} x^n, \end{aligned} \tag{6.11}$$

and

$$\frac{dx}{d\tau} = y + \lambda + x(x-1), \quad \frac{dy}{d\tau} = 0, \tag{6.12}$$

respectively. We call (6.11) the **slow subsystem** since it is a reduced system of equations for the slow system, and similarly, we call (6.12) the **fast subsystem**. The slow subsystem is an **algebraic differential equation** which tells us that the motion of the slow variable y is confined to the curve

$$y = x(1-x) - \lambda. \tag{6.13}$$

We call this constraint for the dynamics of the slow variable the **critical manifold**

$$\mathcal{M}_0(\lambda) = \{(x,y) \in \mathbb{R}^2 : y = x(1-x) - \lambda\}. \tag{6.14}$$

In particular, this is a one-dimensional critical manifold for fixed λ. The critical manifold is a manifold of equilibria for the fast subsystem. If these equilibria are asymptotically stable, then for arbitrarily small ε, there exists an **invariant slow manifold**, $\mathcal{M}_\varepsilon$, near $\mathcal{M}_0$, which nearby solutions exponentially approach [11, p. 70-71]. Since this holds for arbitrarily small ε, we can approximate the dynamics of the slow variable by the critical manifold, $\mathcal{M}_0$. It turns out that $\mathcal{M}_0$ has a saddle-node bifurcation. By the tangency condition for a saddle-node bifurcation, we find that

$$\frac{dy}{dx} = 1 - 2x = 0 \implies x = \frac{1}{2}, \tag{6.15}$$

so if we substitute this into (6.13), we obtain the bifurcation point $(1/2, 1/4 - \lambda)$ tangent to the x-direction. So the system becomes unstable when the stable equilibrium point is destroyed in the saddle-node bifurcation. Thus, it is clear that the bifurcation point defines a tipping threshold, and for $m \geq 2$, this tipping threshold does not correspond to a basin boundary since $\boldsymbol{x}_e(\lambda)$ is globally asymptotically stable. In other words, the bifurcation point partitions $\mathcal{M}_0(\lambda)$ into a manifold of stable equilibria for $x < 1/2$ and a manifold of unstable equilibria for $x > 1/2$. We will call the manifold of stable equilibria the stable critical

manifold, $\mathcal{M}_0^s(\lambda)$. Similarly, we will call the manifold of unstable equilibria the unstable critical manifold, $\mathcal{M}_0^u(\lambda)$.

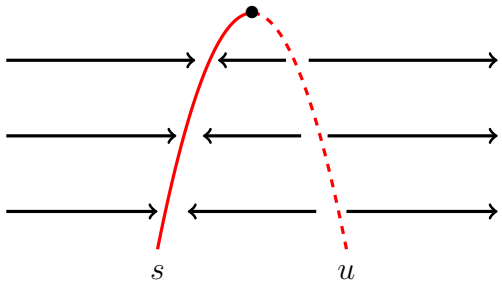

Figure 6.1: The one-dimensional critical manifold $\mathcal{M}_0(\lambda)$, where s represents the stable manifold $\mathcal{M}_0^s(\lambda)$, u represents the unstable manifold $\mathcal{M}_0^u(\lambda)$ and the point on the critical manifold represents the saddle-node bifurcation point (or fold).

6.3 A Steady Drift Approximation

For time-dependent λ, the fast-slow system has quasi-static attractor, $\boldsymbol{x}_e^s(\lambda(t))$. Suppose that the system has steady drift $\dot{\lambda} = \xi > 0$ along the negative y-direction. If we express our equation for the steady drift in terms of the fast-time scale $\tau = t/\varepsilon$, then we see that $\lambda'(\tau) = \varepsilon\xi$, which tells us that λ is a slow variable since ε is very small. Thus, we have fast-slow system with one fast variable and two slow variables.

6.3.1 Reducing the System to Two Variables

The aim of this section is to identify the critical threshold, ξ_c, for which the fast-slow system destabilises. That is, we want to find the value of the steady drift, which if exceeded, leads to trajectories failing to track $\boldsymbol{x}_e^s(\lambda(t))$. We can find this rate by approximating the dynamics of the fast-slow system in the singular limit $\varepsilon \to 0$. We have already seen that consideration of this limit reduces our slow system (6.1) to the slow subsystem (6.11). Since (6.11) is an algebraic differential equation, we can rearrange the algebraic constraint and substitute into

the corresponding differential equation for the slow variable to obtain the **projected slow subsystem**

$$(1-2x)\frac{dx}{dt} = \xi - \sum_{n=1}^{2m+1} x^n, \quad \frac{d\lambda}{dt} = \xi, \tag{6.16}$$

which approximates the dynamics of the fast-slow system on the two-dimensional critical manifold

$$\mathcal{M}_0 = \{(x, y, \lambda) \in \mathbb{R}^3 : y = x(1-x) - \lambda\}. \tag{6.17}$$

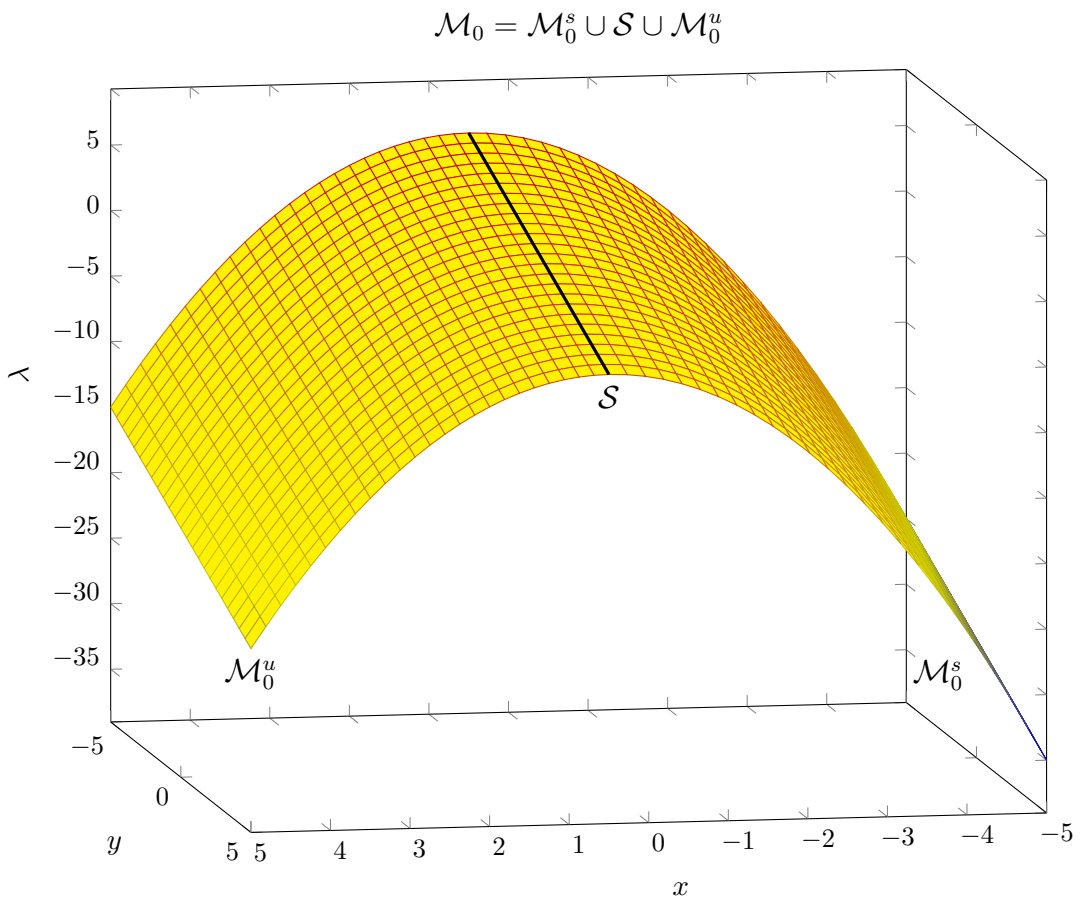

Figure 6.2: The partitioned two-dimensional critical manifold, $\mathcal{M}_0 = \mathcal{M}_0^s \cup \mathcal{S} \cup \mathcal{M}_0^u$. The manifold is separated into three parts, namely a stable critical manifold $\mathcal{M}_0^s$, an unstable critical manifold $\mathcal{M}_0^u$, and a saddle-node bifurcation curve $\mathcal{S}$. $\mathcal{M}_0^s$ is a manifold of stable equilibria and $\mathcal{M}_0^u$ is a manifold of unstable equilibria.

Notice that the projected slow subsystem is singular at $x = 1/2$, that is along the saddle-node bifurcation curve

$$\mathcal{S} = \left\{(x, y, \lambda) \in \mathbb{R}^3 : x = \frac{1}{2},\ y = \frac{1}{4} - \lambda\right\}. \tag{6.18}$$

In other words, $\dot{x} \to \infty$ as $x \to 1/2$, meaning when trajectories $x(t)$ reach $\mathcal{S}$, they diverge to infinity in finite time t. We call this **blow-up** phenomena [7, p. 400]. However, there are special points on $\mathcal{S}$ where the projected slow subsystem is not singular. Such points are called **folded singularities** [14, p. 2842-2843] or **canard points** [24, p. 1256], and occur when $\dot{x} = 0$ on $\mathcal{S}$. In this case, the projected slow subsystem has folded singularity given by

$$\left.\frac{dx}{dt}\right|_{x=1/2} = 0 \implies \xi = \sum_{n=1}^{2m+1} \left(\frac{1}{2}\right)^n. \tag{6.19}$$

Therefore, when $\xi = \sum_{n=1}^{2m+1}(1/2)^n$, there exist folded singularities on $\mathcal{S}$ such that $\dot{x}$ remains finite when trajectories reach $\mathcal{S}$.

6.3.2 The Desingularised System

To obtain a phase portrait for the projected slow subsystem, we must apply a transformation so that (6.16) is not singular at $x = 1/2$. It turns out that if we rescale time such that

$$\frac{dt}{d\tau} = 1 - 2x, \tag{6.20}$$

then we have a transformation which transforms the projected slow subsystem so that it is no longer singular along the saddle-node bifurcation curve [23, p. 6]. It is worth noting that time is preserved along the stable critical manifold, $\mathcal{M}_0^s$, but reversed along the unstable critical manifold, $\mathcal{M}_0^u$, since (6.20) becomes negative for $x > 1/2$. This transformation yields

the **desingularised system**

$$\begin{aligned} \frac{dx}{d\tau} &= \xi - \sum_{n=1}^{2m+1} x^n, \\ \frac{d\lambda}{d\tau} &= (1-2x)\xi, \end{aligned} \tag{6.21}$$

where to obtain λ', we have just used the chain rule i.e. $\lambda' = \dot{\lambda}t'$. The desingularised equation for x has an equilibrium point at

$$\xi = \sum_{n=1}^{2m+1} x^n, \tag{6.22}$$

so since there is a saddle-node bifurcation at $x = 1/2$, for $0 < \xi < \sum_{n=1}^{2m+1}(1/2)^n$, all trajectories initially conditioned on the stable critical manifold, $\mathcal{M}_0^s$, will converge to the equilibrium point, x_e, satisfying $\sum_{n=1}^{2m+1} x_e^n$. In other words, trajectories track the quasi-static attractor provided that $0 < \xi < \sum_{n=1}^{2m+1}(1/2)^n$. However, if $\xi > \sum_{n=1}^{2m+1}(1/2)^n$, then trajectories initially conditioned on $\mathcal{M}_0^s$ move towards the saddle-node bifurcation curve at $x = 1/2$ and are no longer constrained to the critical manifold, and so diverge from the quasi-static attractor in the direction of the fast-variable x. The reason why trajectories diverge in this direction away from the quasi-static attractor is because the quasi-static attractor is fixed in the x-direction by $x = 0$, and so the quasi-static attractor can only move in the (y, λ)-plane.

6.3.3 Summary of Steady Drift Approximation

In summary, the fast-slow system with steady drift tips as a result of rate-dependent tipping when the steady drift is greater than the critical threshold. In other words, in our approximation for $\varepsilon \to 0$, the fast-slow system tips when $\xi > \xi_c = \sum_{n=1}^{2m+1}(1/2)^n$. If we expand the geometric sum, we find the critical threshold to be

$$\boxed{\xi_c = 1 - \left(\frac{1}{2}\right)^{2m+1} \ (m \in \mathbb{N}).} \tag{6.23}$$

6.4 Steady Drift Analysis: The Presence of a Hopf Bifurcation

It turns out that numerical simulation reveals for steady drift slightly greater than ξ_c, as defined in (6.23), trajectories spiral around near the saddle-node bifurcation curve, and so trajectories stay near the quasi-static attractor [8, p. 5]. This is due to the presence of a Hopf bifurcation at $\xi = \xi_c$, which we will now show.

We can reduce the system to an autonomous co-moving coordinate system by setting $\eta(t) = y(t) + \lambda(t)$. This change of variables yields the autonomous system

$$\begin{aligned} \varepsilon\frac{dx}{dt} &= \eta + x(x-1), \\ \frac{d\eta}{dt} &= \xi - \sum_{n=1}^{2m+1} x^n, \end{aligned} \tag{6.24}$$

which has equilibrium point (x_e, η_e) satisfying

$$\begin{aligned} \eta_e &= x_e(1-x_e), \\ \xi &= \sum_{n=1}^{2m+1} x_e^n, \end{aligned} \tag{6.25}$$

provided that $\xi = \sum_{n=1}^{2m+1} x_e^n$ has real solutions (since $x, \eta \in \mathbb{R}$). To confirm this equation does in fact have real solutions, we can set $f(x_e) = \sum_{n=1}^{2m+1} x_e^n$ and $f = \xi$. As a consequence of $2m+1$ being odd for $m \in \mathbb{N}$, $f(x_e)$ must be a polynomial of odd degree. Thus, as $x_e \to \pm\infty$, $f(x_e) \to \pm\infty$ respectively. Furthermore, due to polynomials being continuous everywhere, this tells us that $f(x_e)$ intersects the x_e-axis at least once. Recall that we can rewrite $f(x_e)$ as

$$f(x_e) = \frac{x_e(1-x_e^{2m+1})}{1-x_e} \tag{6.26}$$

for $x_e \neq 1$. From this, it is evident that the only solution to $f(x_e) = 0$ is $x_e = 0$. However, this form of $f(x_e)$ does not hold for $x_e = 1$, so we must evaluate the original polynomial at this value. If we do this, we find that $f(1) > 0$. Therefore, $f(x_e)$ has a single real root,

namely $x_e = 0$. It is clear from figure 6.3 that the line $h = \xi$ can always intersect $f(x_e)$ at least once. Thus, the equation $\xi = \sum_{n=1}^{2m+1} x_e^n$ has real solutions, and so the system has equilibrium point (x_e, η_e).

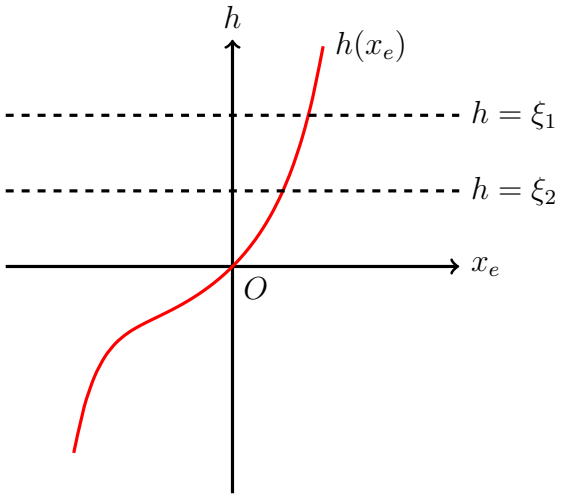

Figure 6.3: A sketch of $f(x_e)$ with intersecting straight lines for arbitrary values of ξ.

The Jacobian matrix of (6.24), evaluated at the equilibrium point (x_e, η_e), is given by

$$\boldsymbol{J}(x_e, \eta_e) = \begin{bmatrix} 1/\varepsilon(2x_e - 1) & 1/\varepsilon \\ -\sum_{n=1}^{2m+1} n x_e^{n-1} & 0 \end{bmatrix}, \tag{6.27}$$

which has trace and determinant

$$\operatorname{tr} \boldsymbol{J}(x_e, z_e) = \frac{1}{\varepsilon}(2x_e - 1) \quad \text{and} \quad \det \boldsymbol{J}(x_e, z_e) = \frac{1}{\varepsilon} \sum_{n=1}^{2m+1} n x_e^{n-1}. \tag{6.28}$$

By using the trace and determinant, we can construct the characteristic polynomial for the Jacobian matrix:

$$\gamma^2 - \frac{1}{\varepsilon}(2x_e - 1)\gamma + \frac{1}{\varepsilon} \sum_{n=1}^{2m+1} n x_e^{n-1} = 0. \tag{6.29}$$

The characteristic polynomial has eigenvalue solutions given by

$$\gamma_{\pm} = \frac{1}{2\varepsilon}\left[2x_e - 1 \pm \sqrt{(1-2x_e)^2 - 4\varepsilon \sum_{n=1}^{2m+1} n x_e^{n-1}}\right]. \tag{6.30}$$

Clearly, for $x_e < 1/2$, the eigenvalues have negative real part. This means that the equilibrium point is asymptotically stable, which means the system tracks the quasi-static attractor for $\xi < \xi_c$. This is consistent with our earlier analysis. However, when $x_e = 1/2$ and $\xi = \xi_c$, we have the eigenvalues

$$\gamma_{\pm} = \pm 2i\left[\frac{1}{\varepsilon}\left(1 - \frac{3+2m}{2^{m+2}}\right)\right]^{1/2}, \tag{6.31}$$

where we have made use of the result

$$\sum_{n=1}^{2m+1} n\left(\frac{1}{2}\right)^{n-1} = 4 - \frac{3+2m}{2^{2m}} \tag{6.32}$$

to express the eigenvalues without a summation. The eigenvalues we have obtained are a pair or purely imaginary complex conjugates. So the eigenvalues cross the imaginary axis when $x_e = 1/2$, and thus the system has a Hopf bifurcation when $\xi = \xi_c$. In other words, when $\xi > \xi_c$, the equilibrium point (x_e, z_e) becomes unstable in a Hopf bifurcation. It can be shown that this is in fact a supercritical Hopf bifurcation [9, p. 18-19]; so there exists a stable limit cycle for which trajectories approach.

Therefore, we have shown that the true dynamics of the fast-slow system behaves very differently to how our approximation in the singular limit $\varepsilon \to 0$ behaves. Due to the presence of a supercritical Hopf bifurcation, trajectories spiral around the saddle-node bifurcation curve. This occurs at the critical threshold, ξ_c, which we found when considering the singular limit $\varepsilon \to 0$. The presence of a Hopf bifurcation is due to $\gamma \propto 1/\varepsilon$. Since the dynamics for the system is modelled by $e^{\gamma t}$ in our linearisation, the rate of the dynamics depends on γt. Thus, we have identified the presence of a third time scale, $T = t/\sqrt{\varepsilon}$.

The reason we were not able to identify this time scale when approximating the dynamics

of the system with the singular limit, $\varepsilon \to 0$, is because this limit approximates the slow dynamics for the system. The exact slow dynamics exponentially approaches the slow manifold, $\mathcal{M}_\varepsilon$, which has the form $x = h(y, \varepsilon)$ [3, p. 1-4]. If we Taylor expand $x = h(y, \varepsilon)$ near $\varepsilon \to 0$, we obtain

$$h(y, \varepsilon) = h(y, 0) + \varepsilon \frac{\partial h}{\partial \varepsilon}(y, 0) + \varepsilon^2 \frac{\partial^2 h}{\partial \varepsilon^2}(y, 0) + \cdots, \tag{6.33}$$

where $x = h(y, 0)$ defines the critical manifold, $\mathcal{M}_0$. Since (6.33) is an expansion in integer powers of ε, the terms involving $1/\sqrt{\varepsilon}$ are not acknowledged, and so the existence of the third time scale, $T = t/\sqrt{\varepsilon}$, is neglected. Therefore, the existence of a Hopf bifurcation is ignored when considering the singular limit $\varepsilon \to 0$.

6.5 Unsteady Drift Analysis

Let us suppose that the quasi-static drift is non-uniform so that it has the form

$$\frac{d\lambda}{dt} = \rho e^{-\lambda}, \tag{6.34}$$

where $\rho > 0$. By means of integration, we find that

$$\lambda(t) = \log(\rho t + A), \tag{6.35}$$

where A is an arbitrary constant and log is used to denote the natural logarithm. If we invoke an initial condition at $t = t_0$, it follows that

$$A = e^{\lambda(t_0)} - \rho t_0, \tag{6.36}$$

and so we have

$$\lambda(t) = \log\left[\rho(t - t_0) + e^{\lambda(t_0)}\right], \tag{6.37}$$

which is a form of logarithmic growth. In the singular limit $\varepsilon \to 0$, the fast-slow system reduces to the projected slow subsystem

$$\begin{aligned}(1-2x)\frac{dx}{dt} &= \rho e^{-\lambda} - \sum_{n=1}^{2m+1} x^n, \\ \frac{d\lambda}{dt} &= \rho e^{-\lambda}.\end{aligned} \tag{6.38}$$

Due to the algebraic constraint we obtain by considering the singular limit $\varepsilon \to 0$, this system must approximate the dynamics of the slow variables x and λ on the two dimensional critical manifold, as defined in (6.18). We know from our steady drift approximation that the projected slow subsystem is singular along the saddle-node bifurcation curve, except at folded singularities. In this case, (6.38) has folded singularity given by

$$\left.\frac{dx}{dt}\right|_{x=1/2} = 0 \implies \lambda(\rho) = -\log\left[\frac{1}{\rho}\left(\frac{2^{2m+1}-1}{2^{2m+1}}\right)\right] \ \forall \rho > 0. \tag{6.39}$$

Therefore, $\dot{x}$ remains finite as $x \to 1/2$, provided trajectories pass through the point $(1/2, \lambda(\rho))$ on the saddle-node bifurcation curve, for $\lambda(\rho)$ as defined in (6.39).

Reminiscent of our analysis for the steady drift approximation, we can rescale time with $t' = 1-2x$ to obtain the desingularised system

$$\begin{aligned}\frac{dx}{d\tau} &= \rho e^{-\lambda} - \sum_{n=1}^{2m+1} x^n, \\ \frac{d\lambda}{d\tau} &= \rho(1-2x)e^{-\lambda}.\end{aligned} \tag{6.40}$$

Along the saddle-node bifurcation curve, the desingularised system has equilibria $(x_e, \lambda_e(\rho))$, where

$$x_e = \frac{1}{2}, \quad \lambda_e(\rho) = -\log\left[\frac{1}{\rho}\left(\frac{2^{2m+1}-1}{2^{2m+1}}\right)\right] \ \forall \rho > 0, \tag{6.41}$$

which are the same as the folded singularities for the projected slow subsystem. Thus, equilibria in the desingularised system are equivalent to folded singularities in the projected

slow subsystem.

The system (6.40) has Jacobian matrix

$$\boldsymbol{J}(x,\lambda) = \begin{bmatrix} -\sum_{n=1}^{2m+1} nx^{n-1} & -\rho e^{-\lambda} \\ -2\rho e^{-\lambda} & -\rho(1-2x)e^{-\lambda} \end{bmatrix}, \tag{6.42}$$

which evaluated at $(x_e, \lambda_e(\rho))$ gives us

$$\boldsymbol{J}(x_e,\lambda_e(\rho)) = \begin{bmatrix} 4-(3+2m)/2^{2m} & (1-2^{2m+1})/2^{2m+1} \\ (1-2^{2m+1})/2^{2m} & 0 \end{bmatrix}. \tag{6.43}$$

It is evident from (6.42) that

$$\det \boldsymbol{J}(x_e,\lambda_e(\rho)) = -\frac{(1-2^{2m+1})^2}{2^{4m+1}} < 0, \tag{6.44}$$

which means that these equilibria are saddles or **saddle equilibria** for the desingularised system. Since equilibrium points in the desingularised system correspond to folded singularities in the projected slow subsystem, we call saddle equilibria for the desingularised system **folded-saddle singularities** in the projected slow subsystem [24, p. 1266].

In most cases, the critical threshold, ρ_c, for the system can only be found numerically. However, it turns out that for initial conditions (x_0, λ_0), which lie on the stable critical manifold, $\mathcal{M}_0^s$, and are sufficiently close to the saddle equilibrium, we can approximate ρ_c by a straight line passing through the saddle equilibrium, with the same direction as the eigenvector corresponding to the stable eigendirection of the saddle equilibrium [24, p. 1260-1261]. If we choose not to simplify summations, we can rewrite the Jacobian (6.43) as

$$\boldsymbol{J}(x_e,\lambda_e(\rho)) = \begin{bmatrix} -\sum_{n=1}^{2m+1} n(1/2)^{n-1} & -\sum_{n=1}^{2m+1}(1/2)^n \\ -2\sum_{n=1}^{2m+1}(1/2)^n & 0 \end{bmatrix} = \begin{bmatrix} -2\beta & -\alpha \\ -2\alpha & 0 \end{bmatrix}, \tag{6.45}$$

where $\alpha = \sum_{n=1}^{2m+1}(1/2)^n$ and $\beta = \sum_{n=1}^{2m+1} n(1/2)^n$. The characteristic polynomial is given by

$$\gamma^2 + 2\beta\gamma - 2\alpha^2 = 0, \tag{6.46}$$

which has eigenvalue solutions

$$\gamma_\pm = -\beta \pm \sqrt{\beta^2 + 2\alpha^2}. \tag{6.47}$$

The eigenvector, $\boldsymbol{v} = (v_1, v_2)^T$, which corresponds to the stable eigendirection of the saddle equilibrium can be found by considering the negative eigenvalue, that being γ_-. To find this eigenvector, we must solve the equation

$$\big[\boldsymbol{J}(x_e, \lambda_e(\rho)) - \gamma_- \mathbb{I}\,\big]\boldsymbol{v} = \boldsymbol{0}. \tag{6.48}$$

Seeking solutions to this equation yields

$$v_1 = \frac{1}{2}\left[\frac{\beta}{\alpha} + \sqrt{\left(\frac{\beta}{\alpha}\right)^2 + 2}\,\right] v_2, \tag{6.49}$$

which, when setting $v_2 = 1$, gives us the eigenvector

$$\boldsymbol{v} = \left(\frac{1}{2}\left[\frac{\beta}{\alpha} + \sqrt{\left(\frac{\beta}{\alpha}\right)^2 + 2}\,\right], 1\right)^T. \tag{6.50}$$

We can approximate the critical threshold, ρ_c, using Wieczorek *et al.* [24, p. 1261, eqn (4.12)], which for our purposes, reads as

$$\lambda_0 - \lambda_e(\rho_c) = \frac{v_2}{v_1}(x_0 - x_e). \tag{6.51}$$

From this, we find the straight line approximation for the critical threshold to be

$$\rho_c \approx \alpha \exp\left[\lambda_0 + \frac{1-2x_0}{\beta/\alpha + \sqrt{(\beta/\alpha)^2+2}}\right]. \tag{6.52}$$

In summary, if $\rho < \rho_c$, then for initial conditions (x_0, λ_0) on the stable critical manifold, $\mathcal{M}_0^s$, trajectories do not reach the saddle-node bifurcation curve, $\mathcal{S}$, and so track the quasi-static attractor. However, if $\rho > \rho_c$, then just as we saw with the steady drift approximation, trajectories reach $\mathcal{S}$ and diverge from the quasi-static attractor in the direction of the fast-variable x.

7 Conclusions

This project presents an introduction to rate-dependent tipping phenomena. If a dynamical system has external conditions modelled by sufficiently smooth, time-evolving functions, then the system has a time-dependent quantity called a quasi-static attractor, which can be thought of as a moving branch of attractors. For initial conditions within the basin of attraction for the quasi-static attractor, we expect trajectories to track this time-dependent quantity. However, it turns out that the system can tip as a result of rate-dependent tipping. This is where a rapid change in external conditions, exceeding a critical threshold, results in trajectories failing to track the quasi-static attractor. As a consequence, trajectories move towards other distant states in phase space.

In section 3, we derived criteria for a linear system to exhibit rate-dependent tipping. We considered both uniform and non-uniform parameter shifts. In the uniform case, we were able to derive inequalities in terms of a tipping radius. We found criteria for the system to both avoid and exhibit rate-dependent tipping. In the case of non-uniform drift, we arrived at a simplified condition to avoid rate-dependent tipping, but concluded that an optimal condition to avoid rate-dependent was difficult to obtain using the tipping radius approach, since it depends on the properties of $\mathbf{\Omega}$. This suggests that the tipping radius approach is limited when considering non-uniform parameter shifts. However, the inclusion of this approach is mentioned to inform the reader of different methods which can be used to analyse rate-dependent tipping. Further work on tipping radius could include trying to find criteria for non-uniform parameter shifts, where $\mathbf{\Omega}$ is a special type of matrix, such as a diagonal matrix, a triangular matrix, diagonalisable [17, p. 15], ect.

In sections 4 and 5, we considered bifurcation models which exhibited rate-dependent tipping. Throughout these sections, our aim was to find analytic forms for the critical threshold, that being the rate of parameter shift, which if exceeded, induces tipping. In the case where the parameter shift was uniform (steady drift), we were able to find analytic forms for the critical threshold for both the saddle-node normal form and the subcritical Hopf

normal form. In addition, we briefly considered a non-uniform parameter shift (unsteady drift) for the subcritical Hopf normal form. It turns out that it is more troublesome to obtain the critical threshold in this instance, and numerical approximation is required to make progress. This was mentioned to highlight how difficult problems with unsteady drift are in comparison to problems with steady drift.

We showed in section 4.3, that when adopting a tipping radius approach to find criteria for the saddle-node normal form to exhibit rate-dependent tipping, the critical threshold obtained overestimates the analytic form we originally found in (4.16). This overestimation was a consequence of the tipping radius being obtained from the linearised system. In other words, our linear model for tipping radius overestimates the critical threshold for a non-linear system. We found an effective tipping radius by using the critical threshold we initially obtained. This corresponds to the distance between the linearised system and the quasi-static attractor, which if exceeded, induces tipping.

Finally, in section 6, we looked at a fast-slow system with rate-dependent tipping. We approximated the slow dynamics of the system by considering the singular limit, $\varepsilon \to 0$. This approximates the slow dynamics to take place on a critical manifold, $\mathcal{M}_0$. It turns out that the critical manifold has saddle-node bifurcation curve, which partitions the manifold into a stable part and unstable part. If trajectories are initially positioned on the stable part of the critical manifold, then below the critical threshold, trajectories will track the quasi-static attractor. If we exceed the critical threshold, then trajectories will cross the saddle-node bifurcation curve and diverge from the critical manifold. This corresponds to trajectories failing to track the quasi-static attractor.

The critical threshold obtained by considering this singular limit is simply an approximation. In reality, the system behaves differently to what our approximation suggests. This is due to the presence of a Hopf bifurcation. As a consequence of this Hopf bifurcation, instead of trajectories diverging after crossing the saddle-node bifurcation curve, trajectories converge to a stable limit cycle and so stay near the quasi-static attractor. Clearly, an area of further

work for this project is to develop an understanding of rate-dependent tipping induced by the presence of periodic orbits [1]. If we were to better our understanding of this, then we would be able to identify whether trajectories converging to a stable limit cycle correspond to trajectories tracking a quasi-static attractor, or if this corresponds to trajectories failing to track a quasi-static attractor. This distinction is important since in one case, we do not have rate-dependent tipping, and in another case, we do have rate-dependent tipping.

Reflecting on this project, there are two main ways to expand on the material presented. One way is to consider the phenomena of rate-dependent tipping for models from different disciplines. In the case of climate science, there has been research on the rate of global warming and how this can cause a sudden increase in the temperature of peatland (partially decayed vegetation) soil. The idea is that if the rate of global warming is rapid enough, then this could potentially induce a dangerous release of peatland carbon into the atmosphere [24, p. 1261-1265]. An alternative to this is to consider a more rigorous treatment of rate-dependent tipping phenomena. A potential way to do this is to consider properties of **local pullback attractors** when changing the rate of a parameter shift [1].

References

[1] H. M. Alkhayuon and P. Ashwin. Rate-induced tipping from periodic attractors: Partial tipping and connecting orbits. *Chaos: An Interdisciplinary Journal of Nonlinear Science*, **Vol. 28**(**No. 3**):033608, 2018.

[2] P. Ashwin, S. Wieczorek, R. Vitolo, and P. Cox. Tipping points in open systems: bifurcation, noise-induced and rate-dependent examples in the climate system. *Phil. Trans. R. Soc. A*, **Vol. 370**(**No. 1962**):1166–1184, 2012.

[3] E. Benoît, M. Brøns, M. Desroches, and M. Krupa. Extending the zero-derivative principle for slow–fast dynamical systems. *Zeitschrift für angewandte Mathematik und Physik*, **Vol. 66**(**No. 5**):2255–2270, 2015.

[4] R. Bertram and J. E. Rubin. Multi-timescale systems and fast-slow analysis. *Mathematical biosciences*, **Vol. 287**:105–121, 2017.

[5] J. Carr and R. G. Muncaster. The application of centre manifolds to amplitude expansions. ii. infinite dimensional problems. *Journal of differential equations*, **Vol. 50**(**No. 2**):280–288, 1983.

[6] U. Feudel, A. N. Pisarchik, and K. Showalter. Multistability and tipping: From mathematics and physics to climate and brainminireview and preface to the focus issue, 2018.

[7] V. A. Galaktionov and J. L. Vázquez. The problem of blow-up in nonlinear parabolic equations. *Discrete and continuous dynamical systems*, **Vol. 8**(**No. 2**):399–434, 2002.

[8] J. Hahn. Hopf bifurcations in fast/slow systems with rate-dependent tipping. *arXiv preprint arXiv:1610.09418*, 2016.

[9] J. Hahn. *Rate-Dependent Bifurcations and Isolating Blocks in Nonautonomous Systems*. PhD thesis, University of Minnesota, 2017.

[10] D. Hinrichsen and A. J. Pritchard. *Mathematical systems theory I: modelling, state space analysis, stability and robustness*, volume **Vol. 48**. Springer Berlin, 2005.

[11] H. G. Kaper and T. J. Kaper. Asymptotic analysis of two reduction methods for systems of chemical reactions. *Physica D: Nonlinear Phenomena*, **Vol. 165**(**No. 1-2**):66–93, 2002.

[12] B Kaulakys, M Alaburda, and J Ruseckas. Modeling non-gaussian 1/f noise by the stochastic differential equations. In *AIP Conference Proceedings*, volume **Vol. 922**, pages 439–442. AIP, 2007.

[13] A. C. King, J. Billingham, and S. R. Otto. *Differential equations: linear, nonlinear, ordinary, partial*. Cambridge University Press, 2003.

[14] M. Krupa and M. Wechselberger. Local analysis near a folded saddle-node singularity. *Journal of Differential Equations*, **Vol. 248**(**No. 12**):2841–2888, 2010.

[15] T. M. Lenton. Early warning of climate tipping points. *Nature Climate Change*, **Vol. 1**(**No. 4**):201, 2011.

[16] J. D. Murray. Mathematical biology. i: An introduction. ii: Spatial models and biomedical applications. *Interdisciplinary Applied Mathematics*, **Vol. 17**, 2002.

[17] C. G. Perryman. How fast is too fast? rate-induced bifurcations in multiple time-scale systems. 2015.

[18] D. Poole. *Linear algebra: A modern introduction*. Cengage Learning, 2014.

[19] M. H. Protter. *Basic elements of real analysis*. Springer Science & Business Media, 2006.

[20] K. F. Riley, M. P. Hobson, and S. J. Bence. *Mathematical methods for physics and engineering: a comprehensive guide*. Cambridge university press, 2006.

[21] R. Seydel. *Practical bifurcation and stability analysis*, volume **Vol. 5**. Springer Science & Business Media, 2009.

[22] S. H. Strogatz. *Nonlinear dynamics and chaos: with applications to physics, biology, chemistry, and engineering*. Hachette UK, 2014.

[23] H. Wang, T. Vo, and T. J. Kaper. On the existence of and relationship between canards and torus canards in forced slow/fast systems. *arXiv preprint arXiv:1607.02205*, 2016.

[24] S. Wieczorek, P. Ashwin, C. M. Luke, and P. M. Cox. Excitability in ramped systems: the compost-bomb instability. *Proc. R. Soc. A*, **Vol. 467**(**No. 2129**):1243–1269, 2011.